Structural mapping adjacent to the 'Woman-in-White amphibolite' in the Olary Domain, South Australia.

Ashley David Taylor B.Sc.

Department of Geology and Geophysics
The University of Adelaide

This thesis is submitted as partial fulfillment for the Honours Degree of Bachelor of Science

November 1999

GEOLOGY AND GEOPHYSICS

Australian National Grid Reference

(SI 54 - 2)

ABSTRACT

A structural study of Palaeoproterozoic Willyama Supergroup rocks to the southeast of Old Boolcoomata approximately 20 kilometres north of Olary, South Australia, discloses a complex history of deformation. This includes an axial planar S_1 schistosity and several intersecting locally developed subsequent planar fabrics. The main findings support previous unpublished company studies. Structural maps were produced at various scales in areas surrounding the 'Woman-in-White' amphibolite and all available observations were used to form a chronology of events and tectonic model for the geometric and kinematic evolution of the area.

In a domain east of the 'Woman-in-White' amphibolite the S_1 is parallel to the axial plane of a major isoclinal synform closing to the east. S_2 is axial planar to tight to open class 2 and class 1c F_2 folds that trend generally north to northeast. Regionally, and particularly in the vicinity of the 'Woman-in-White' amphibolite, a third deformation is very intensely developed generating two fabrics. The S_3 schistosity is the axial planar fabric to tight to isoclinal F_3 folds trending consistently east-west. The S_3 fabric is also expressed as a crenulation of the S_1 regional schistosity. These pre-Adelaidean structural elements are recognised as comprising the Olarian Deformation.

Fold interference is present on all scales. Olarian deformation events two and three have given the flat lying western limb of the principal F_1 synform a luniform, dome and basin morphology. Type 2 and type 3 interference patterns are the most common in the area mapped. The occurrence of the two interference patterns is due to the variable angle between OD_2 and OD_3 compressions, which is commonly approximately 40° in the west-southwest part of the mapped area.

This work conforms closely in complexity to previous regional studies and has been supplemented by other new investigations of an important northeast-southwest trending shear zone corresponding to OD_3, lying further to the north, and a geochemical investigation of the 'Woman-in-White' amphibolite indicating its probable mantle origin and possible emplacement before all deformations occurred.

TABLE OF CONTENTS

List of Figures

Chapter 1

Chapter 2

Chapter 3

(g) Psammopelitic gneiss with interbedded migmatite showing intense folding. The rock commonly has an interbedded appearance with psammitic and pelitic layers along with migmatite.
(h) Thin section of the albitite unit showing a compositional layering, magnetite-quartz-feldspar, that has been recrystallised.

Chapter 4

Cross section 1
Cross section 2

Figure 4.1 Sub areas with bedding(So) and schistosity (S1) data.
Figure 4.2 Analysis of F2 folds found in a sample of psammopelitic gneiss with interbedded migmatite.
Figure 4.3 Subareas with L2 lineation data.
Figure 4.4
(a) Open F_2 folding in Psammopelitic gneiss with interbedded migmatite unit, plunging east in the interference zone (subarea B).
(b) Tight F_3 fold in Psammopelitic gneiss with interbedded migmatite, plunging east and verging to the north.
(c) Sample containing a small F_3 fold and shearing. The plunge of the fold is defined by the rodding lineation of the migmatite around the rim of the sample.
(d) Fold isogon analysis of the fold from (c). It shows the fold is class 2 (Ramsay and Huber, 1987) with parallel isogons.
(e) Thin section from the limb of the fold in (c). It shows the F_3 axial planar fabric cross cutting the stronger S_1 schistosity.
(f) F3 crenulations in the hinge schist unit plunging east at approximately 20 degrees. Lens cap is approx. 4cm in diameter.
(g) S-C mylonite from the MacDonald Shear Zone.
Figure 4.5 Subareas with L2 lineation data.
Figure 4.6 Deformed lineation loci: lineation geometry arising during folding of an intially planar surface which contained an initially rectilinear structure. X, Y, and Z indicate the principle strain axes of the superposed homogeneous strain, *a* is the slip direction of simple shear in the shear fold and *a*' the modified direction after imposing a homogeneous strain. (Ramsay and Huber, 1987)

Chapter 5

Chapter 6

CHAPTER 1 - Introduction

1.1 Introduction

The region of interest in this study is to the southeast of Old Boolcoomata, and includes the Woman in White, 'Mulga Bore Creek', and Cathedral Rock area, approximately 20 kilometres north of Olary, South Australia. The area is found in the Olary Domain (OD) of the Willyama Complex (Figure 1.1). The area of interest contains very complex geology with evidence of several phases of deformation. It includes the middle part of the Palaeoproterozoic Olary Willyama Supergroup stratigraphy, including the quartzofeldspathic, calcsilicate, Bimba and pelite suites of Clarke *et al*., (1986).

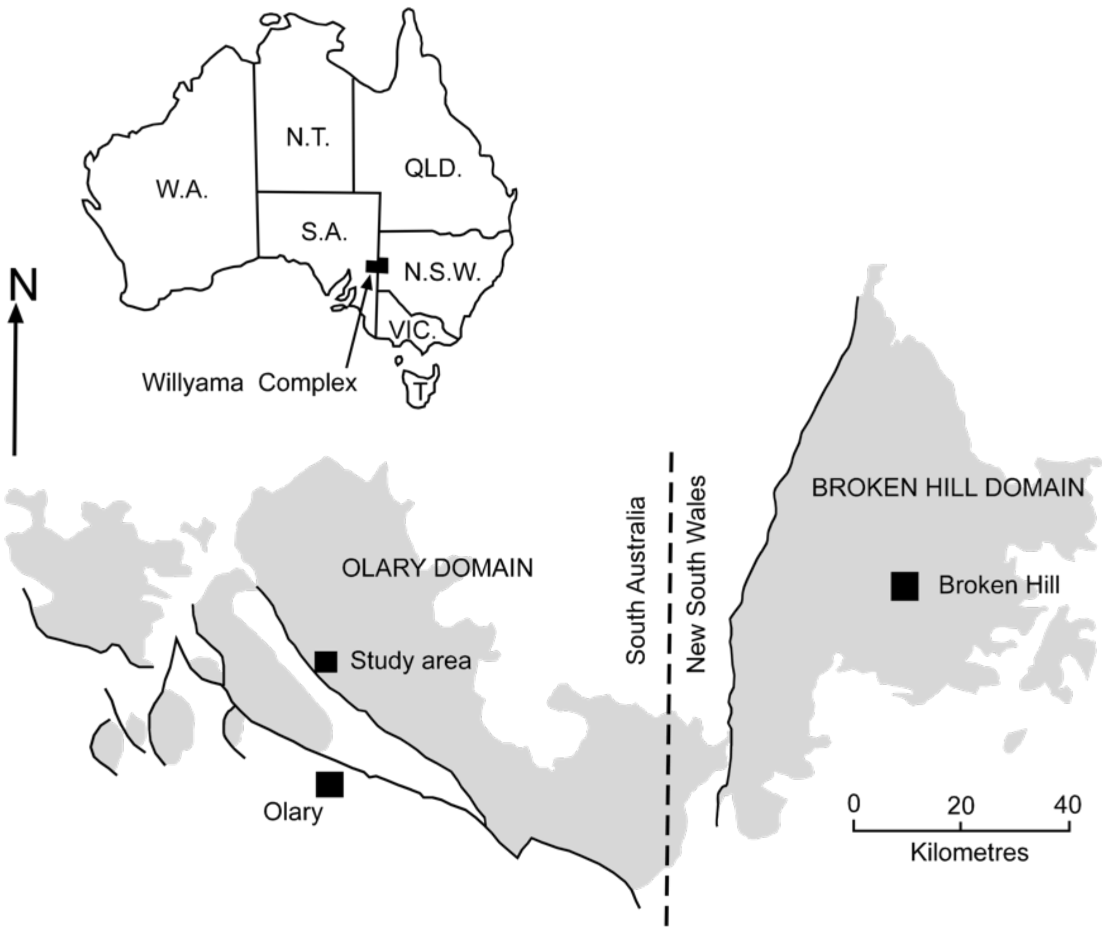

Figure 1.1 Location of the field area within the Willyama Complex.

There is, in addition to metasediments, an assortment of felsic igneous rocks including A-type volcanics (approximately 1710 Ma) and coexisting granites, and Mesoproterozoic granites (Ashley *et al.*, 1998). The 'Woman-in-White amphibolite' is a large amphibolite body that resides in the eastern portion of the area of interest. The study of Archibald (1980) indicates that numerous other amphibolite bodies exist at a similar position in the stratigraphic section and some of these, or even all, may be a segment of the same body that has been dismembered and repeated by folding.

1.2 Polyphase Deformation

The ''Woman-in-White' area is structurally very complex. There is abundant evidence for fold interference. In chapter 5.2 there is a description of how interference patterns are formed by the effects of one deformation being overprinted by another deformation. This can result in folds that are refolded producing fold interference patterns. The angle between the two directions of stress and the angle of the topography will determine the type of pattern seen in the field (Ramsay and Huber, 1987).

1.3 Aims of Study

The aims of this study are;

- To produce detailed structural maps at various scales of the area adjacent to the 'Woman-in-White amphibolite.'
- To analyse major and minor structures of the rocks to develop an understanding of the formation of the area.
- To compare the structural information with the geochemical analysis from Constable (1999) to provide an explanation for the timing of the emplacement of the 'Woman-in-White amphibolite.'
- Use all information to produce a chronology of deformational events and form a tectonic model that explains the geometrical and kinematic evolution of the area.

1.4 Methods

Field work comprised a large part of this project. This included detailed structural mapping centred about the 'Woman-in-White amphibolite' for a period of six weeks beginning on the 1st of May, 1999. Field oriented samples were collected for sectioning and analysis in the laboratory. Horizontal surface sketching, using grids, was carried out to gain information on the structure at smaller scales.

Other analyses carried out included drafting and describing the structural geometry of the area to build a chronology of the relative deformation events. The area has also been examined using the stereographic programme *StereoPlott*© to give further information on the deformation.

Mapping was completed on aerial photographs provided by the Department of Primary Industries and Resources of South Australia. Stereographic photographs at a scale of 1:25 000 were enlarged to 1:10 000 for more detailed mapping to be carried out in the field. Maps were drafted using the computer programme *Freehand*© and three dimensional drawings were generated by *Extreme 3D*©.

CHAPTER 2 - Regional Geology

2.1 Geological Setting

The Olary Domain (OD) is situated in the Curnamona Province which extends across eastern South Australia and western New South Wales, outcropping in the Willyama, Mount Painter and Mount Babbage Inliers. However, most of the province is under sedimentary cover. The Province consists of a sequence of late Palaeoproterozoic metasedimentary and metavolcanic rocks (Willyama Supergroup), and local metamorphosed intrusives, together with early Mesoproterozoic volcanic and sedimentary rocks and granitic intrusives (Ashley *et al.*, 1998). The largest known outcrop in the Curnamona Province is the Willyama Inlier which forms a series of semi-isolated, partly exposed blocks which characteristically have faulted western margins and are unconformably overlain by Adelaidean sediments on their eastern margins. In the South Australian sector, basement is generally referred to as the Olary Block which is physically separated from the Broken Hill Block by a major north-northeast-trending fault (Flint and Parker, 1993).

The Willyama Supergroup has been interpreted as having been deposited in a failed Palaeoproterozoic rift, which was subsequently deformed and metamorphosed. The western margin of the rift, between Mount Robe and Olary, corresponds with the western limit of significant volumes of basic magma. The eastern margin may have been near Broken Hill. However, as a result of deformation, including the formation of regional nappes with overturned limbs, the Broken Hill orebody has been folded into its present position and is now on top of the original crustal fracture that controlled the ascent of the fluids that formed it (Flint and Parker, 1993).

The Olary Block portion of the Willyama Supergroup may represent a rift-margin shelf setting and although a detailed palaeoenvironmental synthesis has not been attempted, the sequence may be consistent with deposition in a lacustrine to marine, including possible sabkha setting, deepening upwards into marine strata. Although coexistent magmatism was largely felsic, there is evidence for bimodality (Ashley *et al.*, 1998).

The OD is mainly composed of low to high grade regionally metamorphosed and deformed late Palaeoproterozoic sedimentary and minor volcanic and intrusive rocks. The

Palaeoproterozoic rocks have been intruded by extensive volumes of early Mesoproterozoic granitoids and scattered mafic dykes of Neoproterozoic age. Data from the Benagerie Ridge (Northern area) imply that the degree of deformation and metamorphism of the OD sequence is less than that to the south. Cover over the OD on the Benagerie Ridge is mostly Cainozoic, but in places includes Cambrian and Adelaidean rocks (Ashley *et al*., 1998).

2.2 Stratigraphy

The OD consists of two major groups of metasediments. They are the Willyama Complex deposited during the Palaeoproterozoic and the younger rocks of the Adelaidean Supergroup deposited in the Neoproterozoic.

2.2.1 Willyama Supergroup

The Willyama Supergroup is separated into five major suites that have been correlated with the Broken Hill Domain (Figure 2.1).

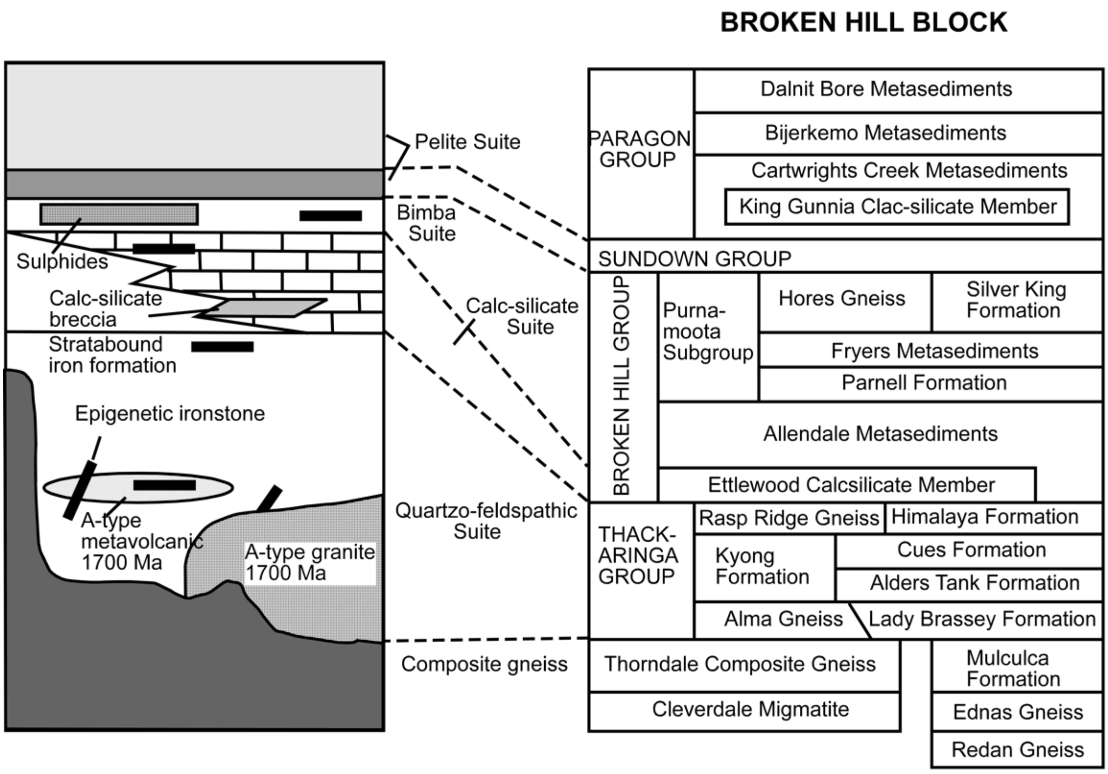

Figure 2.1 Interpreted correlation of the Willyama Supergroup sequence in the Olary Domain with the Broken Hill Domain (Ashley et al., 1998).

The five suites are;

Composite gneiss suite (CGS)

Flint and Parker (1993) consider the CGS as the basal unit in the Olary Block. It consists of coarse grained and migmatitic quartz-feldspar-biotite ± sillimanite ± garnet gneiss. Plagioclase-quartz laminae and microcline-rich pegmatitic segregations are abundant, and stratiform quartz-biotite-magnetite (± sulphide, amphibole, garnet, apatite) rocks, mafic gneiss, sillimanite-garnet schist and quartzite are occasionally present.

Quartzofeldspathic gneiss suite (QGS)

The QGS includes interbedded, medium grained, albitic psammites and pelites, but also includes felsic volcanic or epiclastic lenses and minor magnetite ± barite-bearing horizons, which are considered to be exhalative in origin. The upper part of the QGS is marked by greater lithological variability, with a thick migmatitic pelite unit (middle schist), thick quartz-albite horizons, and quartzite units which are locally ferruginous. (Ashley *et al*., 1998).

Calcsilicate suite (CS)

The CS shows considerable lateral and vertical lithological variability with epidotitic calcalbitites, fine grained quartz-albite metasediments, and medium grained psammopelitic schists. There are also felsic volcanic lenses, which are the highest volcanogenic rocks to date recognised below the 'pelite suite'. Locally black staining, near the top of the unit, indicates manganese enrichment, occasionally shown by the presence piemontite (Ashley *et al*., 1998).

Bimba Formation

The Bimba Formation is characterised by quartz-biotite-albite ± muscovite ± sillimanite metasiltstone interlayered with marble, laminated marble, albitic chert and calcsilicate gneiss. The unit reaches a thickness of 50m in some areas, and is laterally continuous, finely laminated and host to mainly pyritic sulphides (Flint and Parker, 1993). The unit is often marked by the presence of gossans.

Pelite Suite (PS)

In the outcropping region of the OD, the PS is dominated by pelitic and psammopelitic schist (biotite-muscovite-quartz ± Al silicates ± garnet ± tourmaline), locally grading into thin psammites higher in the sequence. A noticeable graphitic facies commonly occurs towards the base of the unit (Ashley *et al*., 1998).

2.2.2 Adelaidean Supergroup

The Adelaidean Supergroup is mostly represented by the Burra Group and the Umberatana Group. The Burra Group consists of polymictic conglomerates, quartzite, marble and siltstone. The unconformity between the Adelaidean Supergroup and the Willyama Supergroup is usually marked by the conglomerate (Ashley *et al*., 1998).

2.3 Deformation

Summary of Deformation interpretations in table 2.1.

The Olary Block has suffered five deformational episodes. The Proterozoic 'Olarian' Orogeny comprises events $OD_{1\text{-}3}$ affecting solely the lower Proterozoic gneisses and events $DD_{4\text{-}5}$ took place during the Cambrian 'Delamerian' Orogeny deforming the upper Proterozoic Adelaidean sequence. Minor crenulation of the 'Olarian' deformation fabrics near contacts of the two sequences and broad warping of the basement are the $DD_{4\text{-}5}$ effects within the gneisses (Clarke *et al*., 1986). There is evidence that there was a metamorphic-deformation event, at least as early as approximately1640-1630 Ma due to the reported presence of foliated metasedimentary schist xenoliths in the I-type granitoid at Poodla Hill (zircon U-Pb age of 1629+12 Ma). Indirectly, an early deformation can also be inferred from the fact that foliated 1710-1700 Ma A-type metagranitoids have been intruded by mafic dykes, which, in

<table>
<tr><th>Berry et al. (1978).</th><th>Clarke et al. (1986)</th><th>Majoribanks et al. (1980)</th></tr>
<tr>
<td rowspan="2">D_3: Folding and retrograde greenschist facies conditions.

S_3: strong mesoscopic crenulation cleavage in more pelitic units. Has redistributed S_1 and S_2. Muscovite crystalised axial planar to F_3.

F_3: open ENE plunging macroscopic folds (60^0 - 70^0).</td>
<td>D_3: Retrograde Shear Zones (Lower amphibolite greenschist facies).

S_3: pre-existing fabrics rotated to parallel with generally steeply south dipping strongly foliated zones.
F_3: near verticle E striking axial surface. Resricted to discrete shear zones.</td>
<td rowspan="2">D_3

S_3: vertical axial planar schistosity.
A result of crenulated older fabrics and retrograde orientated growth of muscovite and chlorite ± biotite.

F_3: small to large scale moderately open folds.</td>
</tr>
<tr>
<td>D_2

S_2: near vertical axial plane defined by moderate to strong crenulations of S_1 (producing L_2)
F_2: meso to macroscopic, upright to reclined, open to tight folds with steeply NW dipping axial surface. Folds trending NE to E</td>
</tr>
<tr>
<td>D_2
S_2: locally weak crenulation resricted to pelitic units concentrated at 120^0.
F_2: open local folding.</td>
<td></td>
<td>D_2

S_2: localised to F_2 hinge zones.
F_2: plunge SW at moderate angles parallel to L_1.</td>
</tr>
<tr>
<td>D_1: Mid amphibolite facies.

S_1: Schistocity and gniessosity parallel to layering and remnant bedding.
F_1: rare mesoscopic isoclinal folds. Syn tectonic granodiorite intrusion.</td>
<td>D_1

S_1: previously shallow to flat lying axial surface defined by micaceous minerals.
L_1: mineral elongation at high angle to fold axes.
F_1: meso to macroscopic, tight isoclinal recumbant folds trending NE to E.</td>
<td>D_1

S_1: well defined schistocity parallel to bedding.
L_1: 30 - 35^0 to the SW
F_1: NE closing synforms and SW closing antiforms.</td>
</tr>
<tr><td></td><td></td><td>Pre S_1 static metamorphism.</td></tr>
</table>

Table 2.1: Summary of tectonic structures and deformational events for the Willyama Supergroup in the Olary and Broken Hill Domains (adapted from Brett, 1998).

turn, have been intruded by the approximately 1600 Ma S-type granitoids (such as in the area south of Triangle Hill) (Ashley *et al*., 1998).

Within the lower Proterozoic metasediments the stratigraphic unit repetition is principally controlled by northeast to east trending, upright, open to tight OD_2 folds, refolding an earlier OD_1 recumbent terrain (Majoribanks et al. 1980). Moderate to strong crenulation of a pre-existing and previously shallow dipping or flat lying fabric is present in most localities. Development of the later near-vertical OD_2 schistosity obliterates much of the earlier fabric in pelitic rocks (Clarke *et al*., 1986). Clarke *et al*., (1986) also suggests the effects of OD_3 are mostly gentle warps of pre-existing fabrics and dissection by retrograde shear zones but have only minor consequence upon stratigraphic unit geometry. F_3 folds suggest compression from the same direction as the retrograde shear zone hence both are part of one event. Berry *et al*., (1978) suggests OD_3 consisted of open upright folds, S3 crenulations, local axial plane schistosity, striking easterly to northeasterly and steep easterly trending retrograde shears.

2.4 Metamorphism

Clarke *et al*. (1987) implied that the pressure-temperature-time (P-T-t) path for the OD is anticlockwise on the basis of the composition of coexisting minerals. The metamorphism related to OD_1 and OD_2 probably reflects a maximum of upper amphibolite grade over much of the OD (Figure 2.2), but probably lower amphibolite grade to the north and greenschist grade on the Benagie Ridge, where the sequence is less deformed (Ashley *et al*., 1998). The metamorphism due to OD_3 (and retrograde shear zones) appears to be low grade, generally containing muscovite (sericite) and/or chlorite, and in some locations biotite, chloritoid and minor garnet (Ashley *et al*., 1998). The two Delamarian deformations (DD_4 and DD_5) occurred under upper-greenschist facies metamorphism. There is no evidence in the region adjacent to the OD for Delamerian metamorphism to have attained garnet grade (Ashley *et al*., 1998).

Based on mineral assemblages the OD has been separated into metamorphic zones (Figure 2.3). The Old Boolcoomata region is situated in the IIb metamorphic zone with andalusite staurolite porphyroblasts dominant.

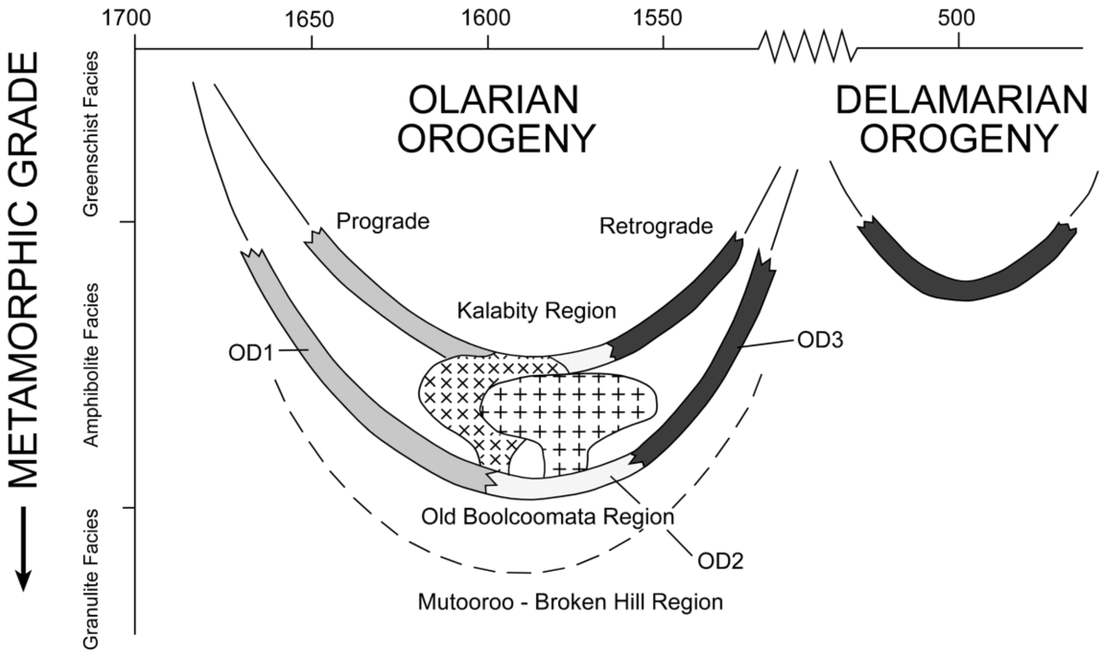

Figure 2.2 Metamorphic grade and timing of the major deformational events for the Olary Domain (Flint and Parker, 1993).

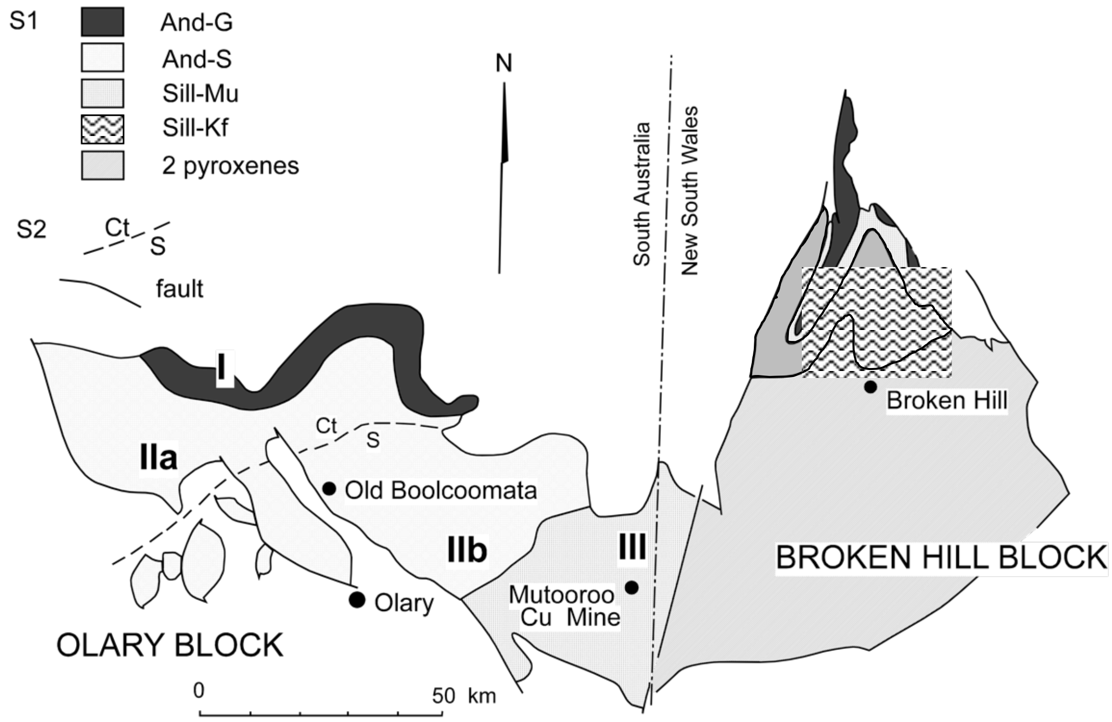

Figure 2.3 Metamorphic assemblages through the Olary and Broken Hill Domains based on porphyroblasts. And-andalusite; G-garnet; S-staurolite; Sill-sillimanite; Mu-muscovite; Kf- k-feldspar. (Clarke et al., 1986).

CHAPTER 3 - Lithological variation and aerial distribution within the area surrounding the 'Woman-in-White amphibolite.'

3.1 Introduction

The following chapter describes the sequences of metasediments from the Willyama Supergroup as well as a brief description of intrusive rocks that crop out in the research area. Lithologies discussed in this chapter relate to the geological map (Figure 3.1) drafted for this study. The 'Woman-in-White' area has good exposure with outcropping rocks abundant. This is rare for the OD which is predominantly under cover. The field area is dominated by Willyama Supergroup rocks with Adelaidean rocks outcropping only in the southwestern section of the map (Figure 3.1).

3.2 Metasediments

Psammopelitic migmatitic gneiss (PG)

This unit only outcrops on the eastern side of a major syncline. This unit contains a strong foliation and hosts an abundance of migmatite. The PG unit is generally medium grained and contains quartz-biotite-muscovite-feldspar ± garnet and magnetite. The unit is continuous reaching a thickness of 200m. The eastern boundary is the contact with the Drew Hill Granite. The contact is generally concordant with the layering.

Interbedded psammopelitic gneiss and albite quartzite (IGA)

This unit is very similar to the older migmatitic unit but contains abundant albite layers and is thickly bedded. Migmatite is present throughout this unit along with pegmatite segregations. Composition is quartz-biotite-albite-muscovite ± magnetite ± epidote. The unit is continuous and outcrops only on the eastern side of the major syncline. Thickness varies from 10-120m. A continuous albite layer (5-20m thick) is present near the eastern boundary of the unit. Some

Figure 3.1

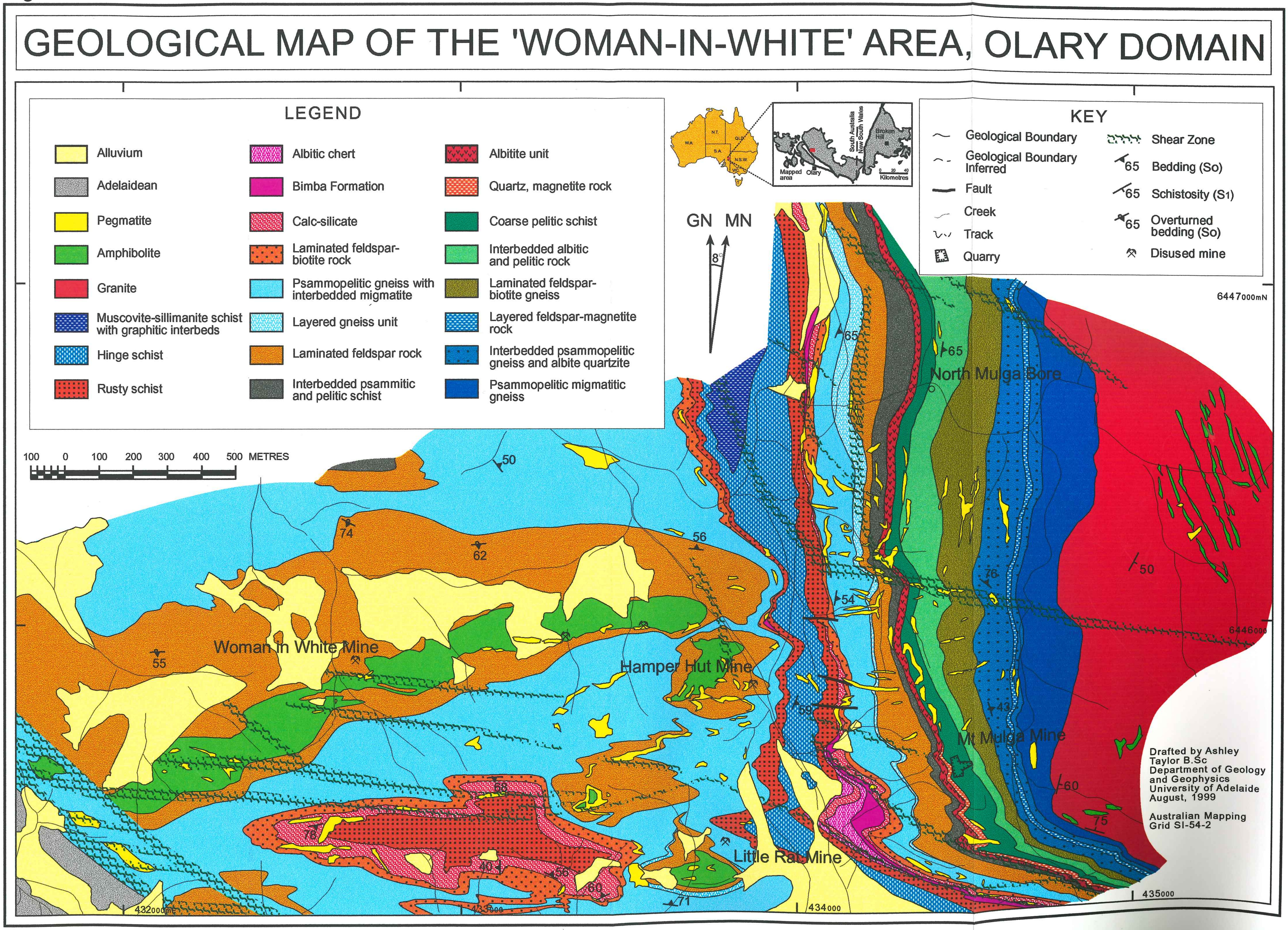
GEOLOGICAL MAP OF THE 'WOMAN-IN-WHITE' AREA, OLARY DOMAIN
LEGEND
Alluvium
Adelaidean
Pegmatite
Amphibolite
Granite
Muscovite-sillimanite schist with graphitic interbeds
Hinge schist
Rusty schist
Albitic chert
Bimba Formation
Calc-silicate
Laminated feldspar-biotite rock
Psammopelitic gneiss with interbedded migmatite
Layered gneiss unit
Laminated feldspar rock
Interbedded psammitic and pelitic schist
Albitite unit
Quartz, magnetite rock
Coarse pelitic schist
Interbedded albitic and pelitic rock
Laminated feldspar-biotite gneiss
Layered feldspar-magnetite rock
Interbedded psammopelitic gneiss and albite quartzite
Psammopelitic migmatitic gneiss
KEY
Geological Boundary
Geological Boundary Inferred
Fault
Creek
Track
Quarry
Shear Zone
Bedding (So)
Schistosity (S1)
Overturned bedding (So)
Disused mine
GN MN
100 0 100 200 300 400 500 METRES
Woman in White Mine
Hamper Hut Mine
Little Rat Mine
North Mulga Bore
Mt Mulga Mine
6447000mN
6446000
432000mE
433000
434000
435000
Mapped area
Olary
South Australia
New South Wales
Broken Hill
Kilometres
Drafted by Ashley Taylor B.Sc
Department of Geology and Geophysics
University of Adelaide
August, 1999
Australian Mapping Grid SI-54-2

areas along this layer become extremely albitised and layering is no longer able to be defined. This unit has a slight amount of magnetite present and it weathers to a buff colour with red tinges in places.

Laminated feldspar-biotite gneiss (LFB)

The LFB unit consists of interbedded quartz-biotite-rich layers with albite-rich massive layers. The albite rich layers weather to a buff yellow colour with red tinges. This unit is very similar to IAP and the boundary is transitional. Migmatites and pegmatite segregations are very common. A fabric is defined by biotite and is more prominent in the schistose layers. Small scale folding is very common. The unit becomes banded in areas that appear to have been sheared. Generally medium grained and contains quartz-biotite-albite ± epidote ± garnet and magnetite. The unit is continuous and reaches a thickness of 200m.

Interbedded albitic and pelitic rock (IAP)

The IAP unit consists of layers of biotite-rich schist interbedded with psammitic albite-rich layers. The psammitic layers weather to a buff colour with reddish tinges in areas. Migmatisation is common between the layers generally concordant with bedding. The rock is generally coarse grained however the biotite rich layers are coarser than the albite rich layers. There is a fabric present in both layers however is much stronger in the pelitic layers. The unit is continuous and only outcrops on the eastern side of the major syncline. This unit ranges in thickness from 40-150m.

Coarse pelitic schist (CP)

This unit is similar to the interbedded psammitic and pelitic schist except is coarser and is more pelitic. Migmatisation is very prominent as are pegmatite segregations. The rock consists of quartz, muscovite, biotite, albite ± tourmaline. Quartz crystals up to 10mm in diameter are present. The unit is again highly sheared in places with possibly some metamorphic regrowth. Compositional layering is not always clearly defined within the unit however there is a strong fabric. Also a crenulation fabric is evident in some outcrops. The unit is continuous with thicknesses ranging from 30 - 100m.

Albitite unit (A)

The albitite unit outcrops as a massive, buff pink to dark red, quartz albite rock varying in grain size from fine to medium. Medium grained magnetite, quartz and albite define layering in the rock (Figure 3.2(h)). The surrounding matrix consists of fine-grained quartz and plagioclase with interspersed magnetite. Quartz eyes up to 5mm in length suggest a volcanic or epiclastic origin. The albite unit forms a continuous layer on the eastern side of the major syncline, ranging in thickness from 2 - 10m.

Interbedded psammitic and pelitic schist (IPP)

This unit is only present on the eastern side of the major syncline. It is a continuous layer ranging in thickness from a few metres to 100m. The schist is generally medium grained and well laminated. It contains quartz, albite, muscovite, biotite and some magnetite. More quartz rich layers and more mica rich layers define the layering. Migmatisation is prominent in this unit. The unit appears to be highly sheared in some areas where banding becomes finer.

Laminated feldspar rock (LFR)

The LFR unit is a fine-grained feldspar-rich rock that weathers to a red colour. In the creeks the unit is buff yellow with pelitic layers also present. The mineralogy of this unit is dominated by albite and quartz, with magnetite ± biotite. It is generally well laminated except in areas of extreme albitisation. Layering consists of coarse-grained quartz, albite and magnetite within a fine grained quartz-albite-magnetite matrix. The unit outcrops as a continuous layer on the eastern limb of the major syncline ranging in thickness from 10-100m. On the western limb of the syncline the unit reaches a thickness of up to 500m, and contains the 'Woman-in-White' amphibolite. At the northern boundary of the 'Woman-in-White' amphibolite an extremely thin and discontinuous albite layer with quartz eyes can be found. The quartz eyes suggest that this thin discontinuous unit may be volcanic in origin.

Figure 3.2

**Due to reordering of section 3.2 this plate has been referred to in the text in reverse order.

(a) Muscovite-sillimanite schist with graphitic interbeds unit in thin section (X-polars). It shows a fabric defined by biotite and muscovite and recrystallised quartz ribbons.

(b) Hinge schist thin section (X-polars) showing a dominant fabric defined by muscovite and minor biotite with weak crenulations.

(c) Bimba Formation showing a strong fabric defined by heavy minerals. The outcrop generally is white (calcareous) however the rock is red to yellow when broken.

(d) Thin section (X-polars) of the Bimba Formation showing the stronger fabric (defined by heavy minerals and biotite) cross-cut by a weaker fabric (defined by magnetite, muscovite, biotite and quartz ribbons).

(e) Outcrop of the calcsilicate unit showing strong laminations with dark red and white layering.

(f) Laminated feldspar-biotite rock outcropping in a creek in the interference zone (subarea B). The fresh rock is grey in colour.

(g) Psammopelitic gneiss with interbedded migmatite showing intense folding. The rock commonly has an interbedded appearance with psammitic and pelitic layers along with migmatite.

(h) Thin section (plane polarised light) of the albitite unit showing a compositional layering, magnetite-quartz-feldspar, which has been recrystallised.

Figure 3.2

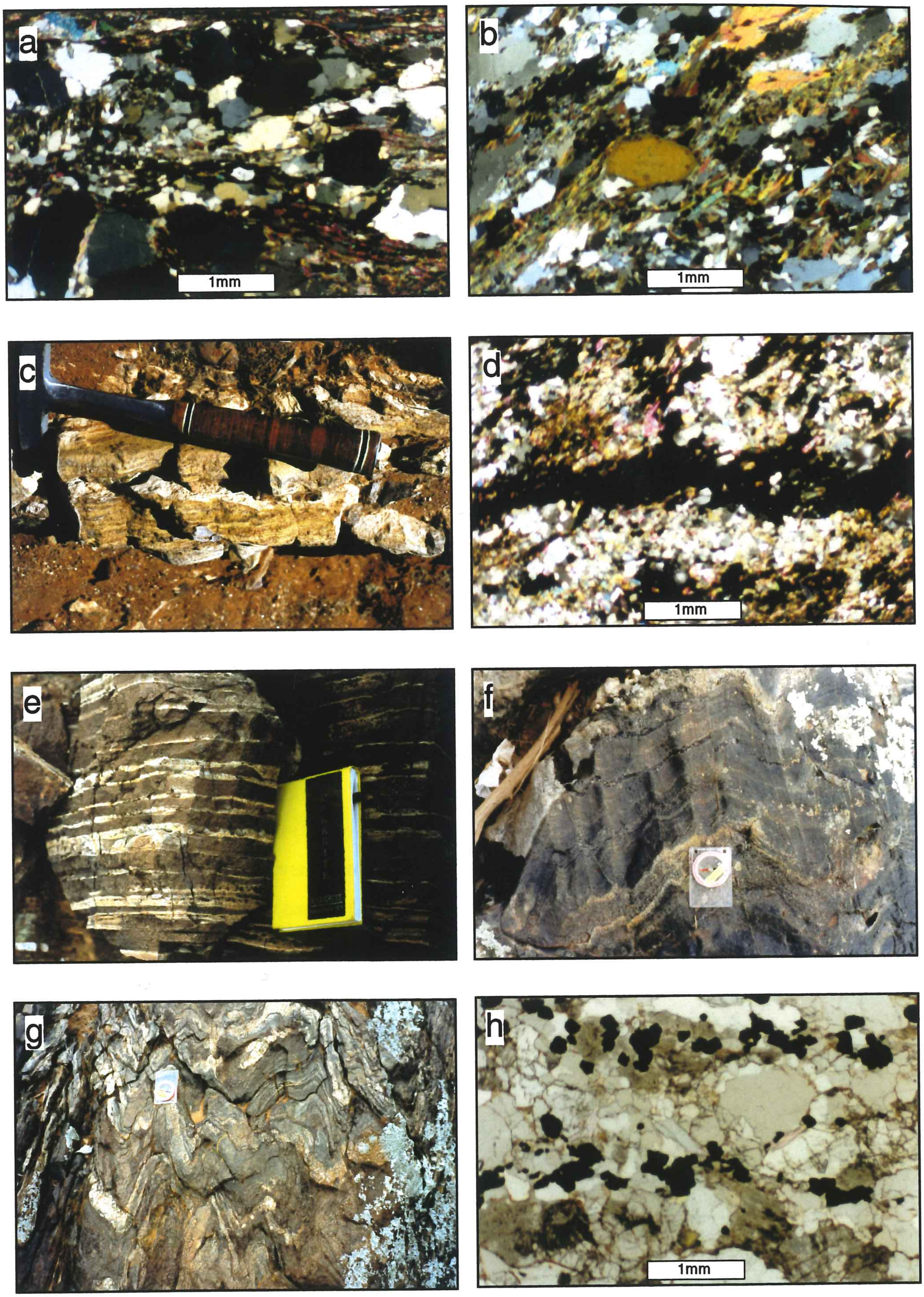

Psammopelitic gneiss with interbedded migmatite (PGM)

The psammopelitic gneiss is an inhomogeneous unit consisting of various interbedded layers overlying the LFR unit (Figure 3.2(g)). In most areas the lithological change is abrupt. The nature of the change is unclear in some areas due to repeated deformation and metamorphism. The unit displays more complex structure than the layered feldspar rocks and calcsilicates. The overall mineralogy includes muscovite, biotite, quartz, feldspar ± sillimanite, andalusite and magnetite. The interbeds consist of psammitic, albitic and pelitic layers of varying thickness. In some areas at the base of the unit exists a discontinuous thinly bedded quartz rich transitional layer up to 80m in thickness (layered gneiss unit on Figure 3.1). The psammitic and pelitic layers contain large retrograde andalusite porphyroblasts up to 1cm in diameter.

The outcrop on the eastern limb of the major syncline is continuous ranging from 30-100m in thickness. On the eastern limb of the syncline the psammopelitic gneiss is the dominant rock type with exposures ranging from 50-400m in thickness.

Laminated feldspar-biotite rock (LFB)

The LFB is generally similar in composition to the older laminated feldspar rock except it contains a higher proportion of biotite. The unit weathers to a distinct red colour. In the creeks the rock is grey in colour (Figure 3.2(f)). Sillimanite porphyroblasts up to 2cm in diameter are also present however the rock is generally fine grained. This unit outcrops as a thin discontinuous layer on the eastern limb of the major syncline reaching a thickness of 40m in some areas. On the western limb the unit is present as small lenses near the hinge of the syncline where it reaches thicknesses of 25m. The unit is also present in the southwest corner of the map area as a continuous layer.

Albitic Chert (AC)

This unit is only present in the southeastern section of the map. It is associated with the calc-silicate unit and contains lenses of that unit. The unit consists of thin bedded to finely laminated feldspar rocks. It weathers to a yellow or buff colour and commonly contains interlayered beds, minor gossan and marble lenses.

Calc-silicate (CS)

The calc-silicate is a laminated to thin bedded rock consisting dominantly of feldspar. Other constituents include epidote, actinolite, magnetite, minor biotite and muscovite ± diopside. The laminations are easily distinguished, with white to cream quartz albite layers ranging from 1-15cm thick and grey to black actinolite, epidote, magnetite ± diopside layers 1-3cm thick (Figure 3.2(e)). The outcrop on the eastern side of the major syncline is discontinuous varying in thickness from 10- 30m. On the western side of the syncline the calc-silicate forms a continuous layer in the southern section of the map. Elongated calc-silicate and micaceous minerals form a tectonic fabric parallel to the laminations. Two intersection lineations are present on most possible bedding surfaces. The calc-silicate unit correlates with the calc-silicate suite described by Clarke *et al*, (1986).

Bimba Formation (BF)

The Bimba Formation is a discontinuous gossanous unit outcropping on the eastern limb of a major syncline. It ranges in thickness from 0-30m. On the western limb of the syncline small gossanous outcrops indicate the stratigraphic location of the Bimba Formation between the rusty schist and calc-silicate units. The unit is a cream to rusty brown colour and is extremely weathered (Figure 3.2(c)). The rock consists of quartz, plagioclase (albite), biotite, muscovite, pyrite and magnetite. Magnetite is enriched within the Bimba (up to 25-30%) and is extremely oxidised giving the rusty brown appearance.

In the Bimba Formation magnetite, biotite and quartz define a fabric (Figure 3.2(d)). Another fabric crosscuts the first at an angle of ~40° and is defined by magnetite, muscovite, biotite and quartz ribbons. Crenulated quartz ribbons are also present. Due to the weathered nature of the Bimba Formation the number of magnetite generations is unclear. This unit corresponds to the Bimba Suite described by Clarke *et al*, (1986).

Rusty schist (RS)

The rusty schist is one of the more iron rich lithologies in the map area. This gives the unit a distinct dark red colour in the field. The rock is relatively coarse grained and contains quartz and sillimanite porphyroblasts. It consists of quartz, feldspar, sillimanite, muscovite ± magnetite and epidote. Strong fabrics are seen in this unit as well as crenulations. The rusty schist outcrops as a continuous unit on the eastern limb of a major syncline, ranging in thickness from 20 to 80m. On the western limb, the rusty schist is the youngest lithology seen and outcrops in the southern section of the map.

Hinge schist (HS)

The hinge schist is generally well bedded. In the creeks the rock is grey with lighter (psammitic) layers and darker (pelitic) layers. Weathered outcrop is similar to that in the creeks except it is a darker shade of grey. The rock consists of quartz, feldspar, biotite, muscovite, magnetite, sillimanite, garnet, tourmaline and graphite (Figure 3.2(b)). Layering is defined by psammitic quartz rich layers and biotite rich pelitic layers, which are commonly separated by migmatite. This suggests a possible variation in water depth at the time of deposition. Calc-silicate ellipsoids are also present in this unit. Their size ranges from a few centimetres up to 50cm in diameter. This unit outcrops as a continuous layer trending north-south in the centre of the map ranging from 30-200m in thickness.

Muscovite-sillimanite schist with graphitic interbeds (MSG)

This unit outcrops in the centre of a major syncline reaching a thickness of 200m in the northern section of the map. It is the youngest of the Willyama Supergroup in the map area. In the field the rock is coarse grained, highly sheared and weathers to a dark brown colour. Melt segregations are abundant. The mineralogy consists of muscovite, sillimanite, quartz, feldspar ± magnetite, graphite and garnet (Figure 3.2(a)). Graphite occurs within interbedded layers and a distinctive graphitic layer marks the base of the unit. Sillimanite porphyroblasts are generally associated with melt segregations.

3.3 Intrusive rocks

'Women-in-White' Amphibolite

The 'Woman-in-White' Amphibolite (WIWA) outcrops on the western side of the major syncline. The weathered nature of the outcrop made it difficult to recognise structures within the rock, however a foliation varying in intensity can be seen. The amphibolite is composed of blue-green-hornblende, plagioclase, quartz, biotite, opaque minerals ± sphene, apatite and rutile. The foliation is defined by the alignment of subhedral to euhedral grains of blue-green hornblende ± biotite and magnetite. Detailed petrologic and geochemical descriptions can be obtained from the study of Constable (1999).

At the eastern end of the outcrop the amphibolite has been folded with the metasediments. This folding event has detached some amphibolite pods from the main body, with one pod showing a contact with migmatitic schist. At the western edge of the outcrop a section of the amphibolite and surrounding calc-albite has been sheared and displaced approximately 200m north, indicating dextral shear movement.

Drew Hill Amphibolite

The Drew Hill Amphibolite (DHA) outcrops throughout the Drew Hill Granite (DHG) from Mulga Bore to the Cathedral Rock area. The DHA is present in the form of dykes that have intruded the DHG. The dykes near Mulga Bore extend up to 400m in length and range from 3-25m in width. Some of the dykes show the effects of large scale boudinage.

The mineralogy consists of hornblende, plagioclase, quartz, opaque mineral ± biotite, epidote and rutile. The dykes generally show a foliation and are medium grained. In hand-specimen one dominant foliation can be seen. Microscopic analysis shows one main fabric and a much weaker second fabric each defined by the alignment of hornblende ± biotite and magnetite.

Drew Hill Granite

The DHG is the large intrusion that occupies the eastern portion of the map area (Figure 3.1). The granite is medium to coarse grained, highly weathered and outcrops have a buff orange colour. Mineralogy consists of quartz, plagioclase, biotite, muscovite, opaque minerals ± hornblende, zircon and sphene. Hornblende is present near the margins of the amphibolite dykes. Constable (1999) suggests this is indicating possible amphibole alteration or a co-magmatic relationship between the DHG and DHA. Some finer grained secondary quartz and plagioclase recrystallisation can be seen in the generally coarse grained DHG.

In the field, one main foliation can be seen. Due to the sparse biotite content only one fabric can be seen in thin section. The fabric is defined by the alignment of biotite and muscovite ± hornblende at contact zones. The fabric in thin section corresponds to the foliation observed in the field. However like the WIWA and DHA two deformational events can be seen.

Pegmatite

Many pegmatite bodies are present in the map area. They range in size from small outcrops to large bodies 150m long. Field evidence shows at least two generations of pegmatite intruding after D_1, and D_2. The post D_2 pegmatite crosscut fabrics due to earlier deformations. Folding of the pegmatite is also common. The mineralogy generally consists of quartz, plagioclase, muscovite and tourmaline. Within the WIWA, large quartz ridges occur with minor plagioclase and tourmaline.

CHAPTER 4 - Structural Analysis

4.1 Introduction

The area surrounding the 'Woman-in-White' amphibolite is structurally very complex. It has undergone the effects of three Olarian deformations as well as Delamarian overprinting. This chapter is devoted to the description of the fabrics and folding of the rocks due to each deformation.

Bedding (S_0) is defined in some layered units by compositional variation. Psammitic quartz-feldspar-rich layers interbedded with pelitic mica-rich layers are interpreted as indicating S_0. Primary structures were difficult to find however one example of cross-bedding was found in the PGM unit. Isolated examples of reverse graded bedding were also found however they were not used as younging criteria as they were inconclusive as younging indicators. In pelite, calc-silicate and albitite units S_0 is not clearly defined. The calc-silcate and albitite units have undergone alteration which in some areas made it difficult to see any layering. In almost all units a layer parallel schistosity is present.

4.2 First Deformation (*O*D_1)

S_1 is a layer parallel schistosity and gneissosity (Figure 4.1). Sillimanite, magnetite, biotite, muscovite and quartz define S_1 in layered units and mica ± heavy minerals define the schistosity in quartz-feldspar-rich units. This fabric is generally parallel to S_0 in the mapped area. The eastern side of the map (subarea E) shows S_1 dipping more shallow than S_0. The difference in the average of S_0 and S_1 readings in this area though is extremely slight (Figure 4.1). In some areas, especially on the western side of the map, S_1 has been severely deformed by overprinting deformations. This has resulted in the stereographic plots for subareas B and C having a dispersed appearance (Figure 4.1).

The S1 layer parallel schistosity is interpreted as the axial planar fabric to a large scale F_1 fold nappe running through the centre of the map (cross section 1). This is a synform with closure to the east. The fold axial trace generally runs north-south however the north and

Figure 4.1. Sub areas with bedding (So) and schistosity (S1) data.

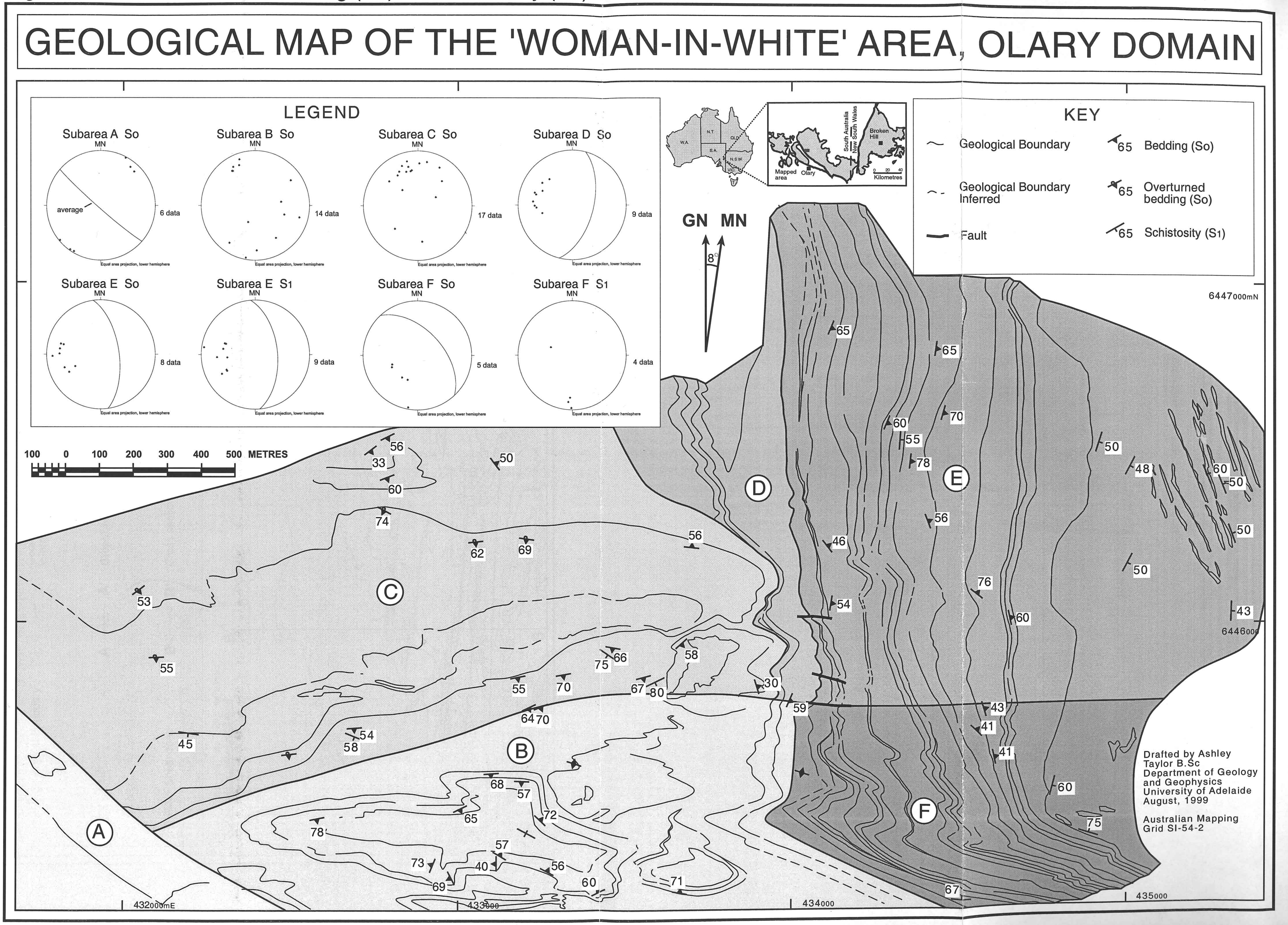

Location of cross sections 1 and 2.

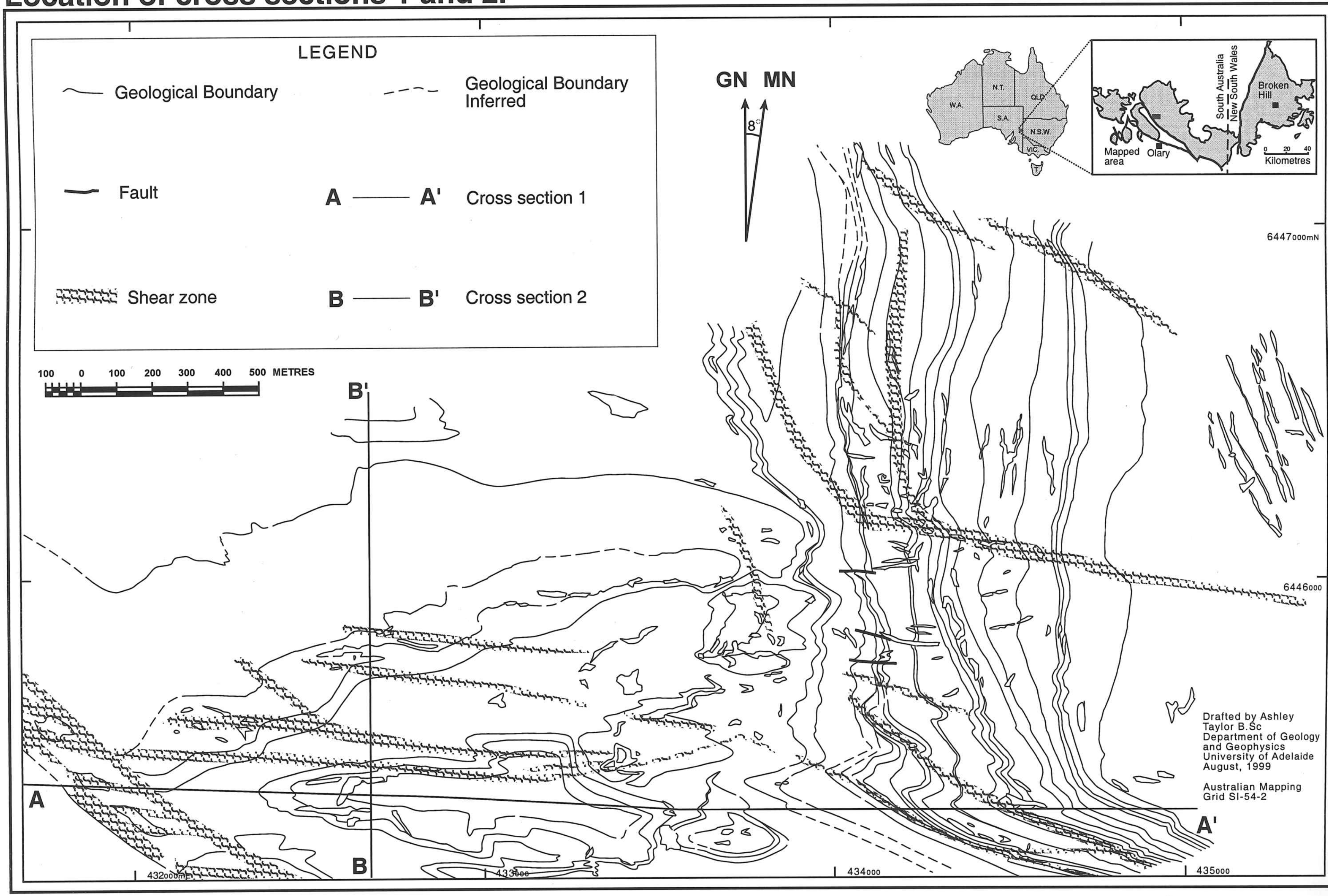

Cross section 1. East - West schematic cross section of the 'Woman-in-White' area

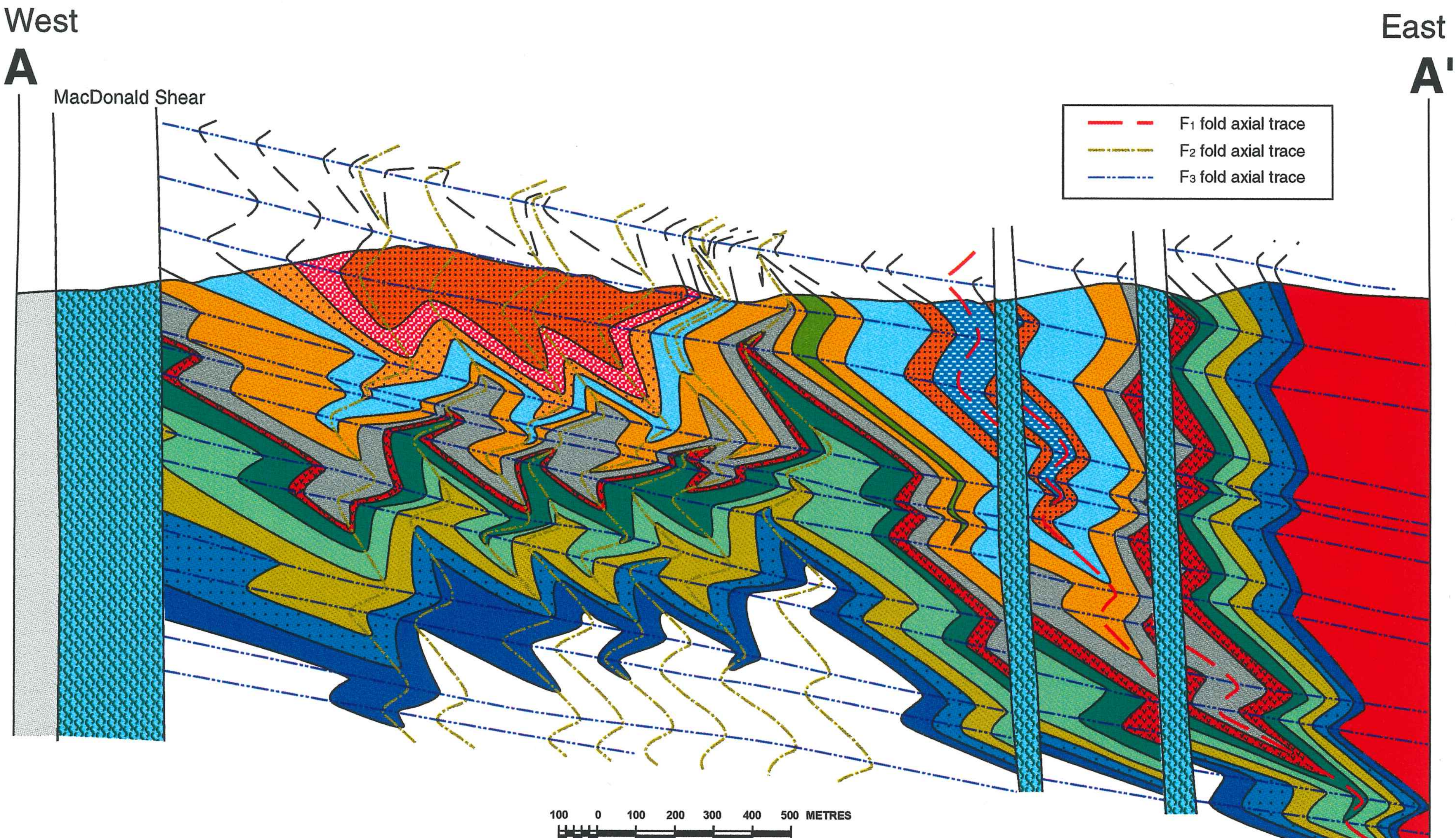

Colours apply to geological map (figure 3.1).

Note: Cross section is highly speculative. Thickness of layers at depth approximate.

south have been sheared to the east. The study of Clark (1999) has a detailed analysis of the synform to the north of the area where it has undergone shearing.

The shape of the outcrop of the MSG unit shows the position of the F_1 fold hinge. The lensing out of this unit is directly due to refolding of the hinge of the F_1 syncline. Archibald (1980) shows the unit outcropping in the southern shear zone (to the south of the mapped area) showing again that the F_1 fold hinge has been refolded.

The eastern side of the F_1 fold axial trace has remained relatively uniform. Bedding is steeply dipping to the east. No younging criteria were found in this area however bedding is interpreted as being overturned (cross section 1). Only in one area other than the main F_1 syncline is there evidence of F_1 folds present in the field area (see section 5.2).

4.3 Second Deformation (*O*D_2)

S_2 is the second foliation seen in the mapped area. It is the axial planar fabric to folds that generally trend to the north-east. Axial planar cleavages and fabrics are widespread, however only in areas of F_2 folds. Subarea E shows the preserved direction of L_2 lineations (plunge of folds and intersection lineations) trending to the north-east. Sillimanite, chlorite, muscovite and biotite define the fabric.

F_2 folds are very common on the western side of the main F_1 fold axial trace (cross section 1). The folds are most commonly class 2 folds (Ramsay and Huber, 1987) with parallel fold isogons however some folds are class 1(c) with convergent isogons. They are generally tight to open (see Figure 4.4(a)). Figure 4.2 shows isogon analysis of F_2 folds from the PGM unit. The orientation of the S_2 fabric, and L_2 lineations, depends upon the position relative to large F_3 folds. In the areas folded by large F_3 folds the orientation of the S_2 fabric tends to be towards the southeast (figure 4.3). L_2 lineations show great plunge variation in the interference zones, however trend consistently to the east in more uniform areas (Figure 4.3). The plunge variation of the F_2 fold hinges is the reason for the interference patterns seen in the southern section of the map.

A common feature of F_2 folds is variation in the scale of the folding. Some areas show large scale folding while other areas show small scale folding. This can be explained as folds

Figure 4.2

Analysis of F2 folds found in a sample of psammopelitic gneiss with interbedded migmatite. The folds are of different class and vary in tightness. The sample also contains a crenulation cleavage due to OD3.

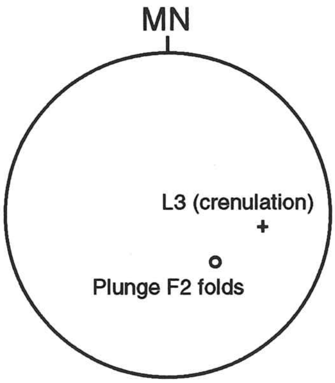

F2 foldin the field (lens cap approx. 4cm)

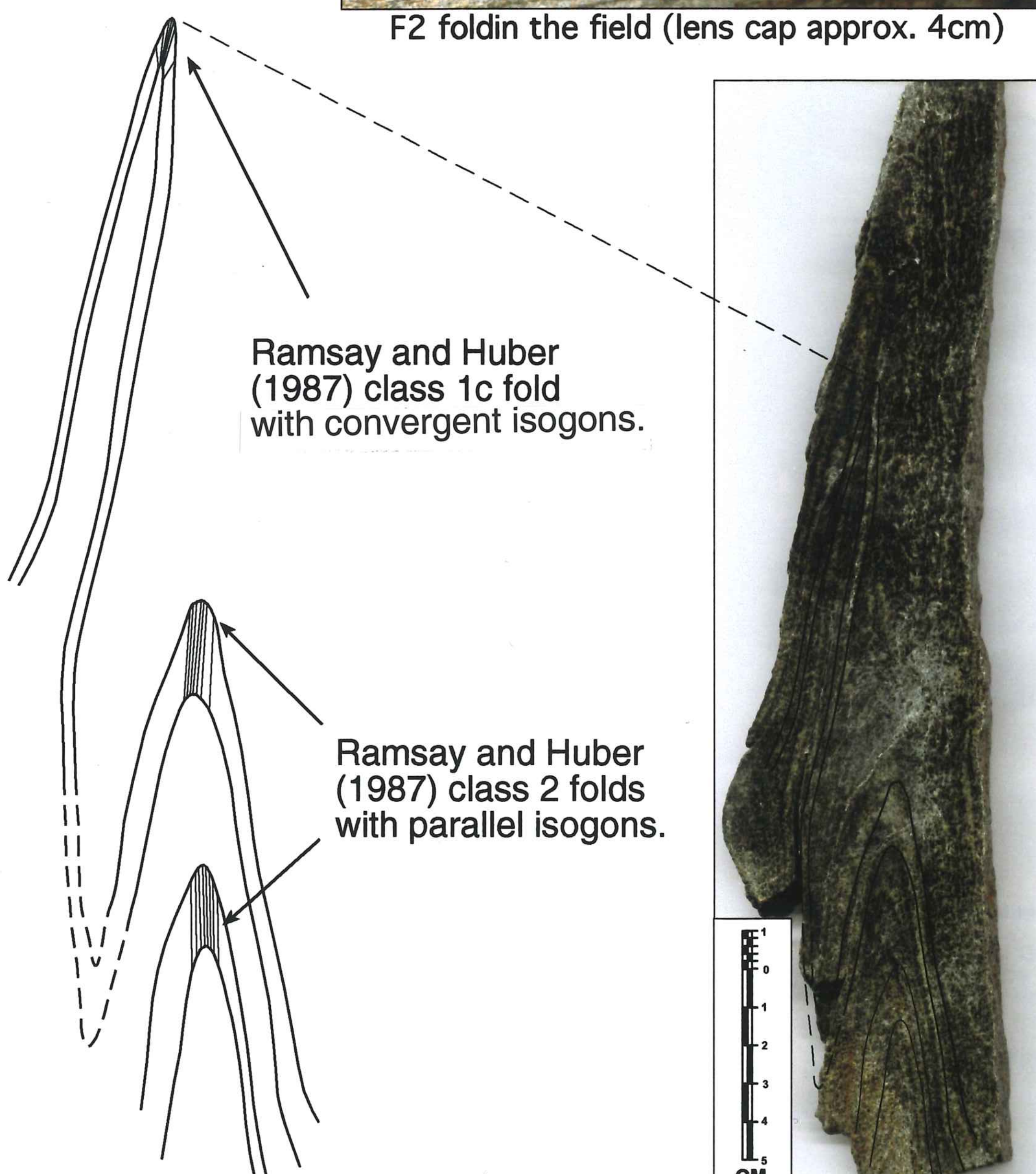

Figure 4.3. Sub areas with L2 lineation data.

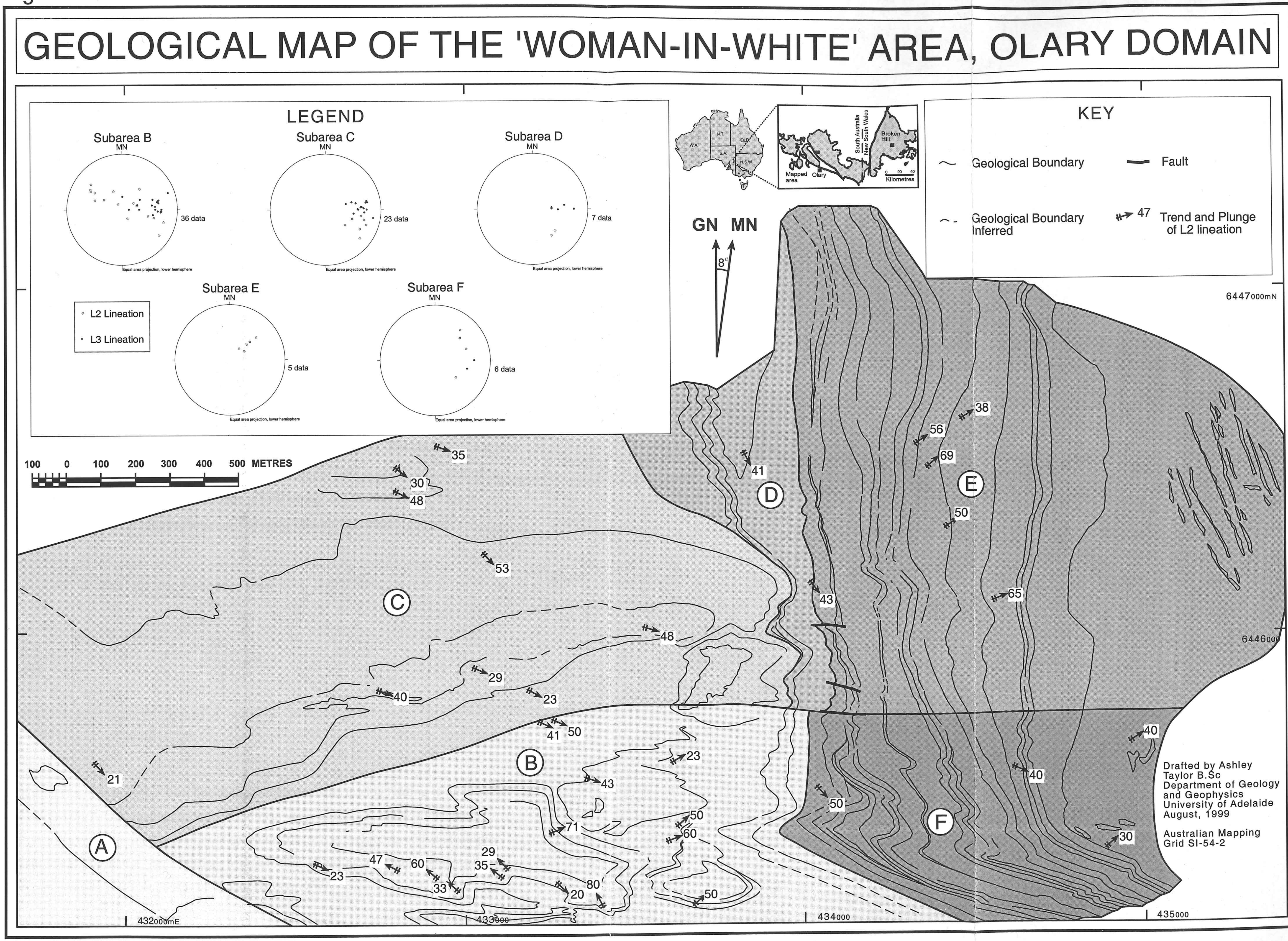

relaying each other in an en-echelon manner (Ramsay and Huber, 1987) with fold hinges dying out (see grid-map, chapter 5).

4.4 Third Deformation (*O*D_3)

The third deformation was very intense for the 'Woman-in-White' area. S_3 is represented by two fabrics. First is the axial planar fabric to F_3 folds (Figure 4.4(e)). This fabric is defined by muscovite and biotite and sometimes chlorite. It trends consistently east-west. The second type of S_3 fabric is a crenulation of the S_1 fabric (Figure 4.4(f)). This fabric is defined by mica minerals and is mostly seen in schistose units.

OD_3 produced tight to isoclinal folds with axes trending to the east. They are generally of class 2 (Ramsay and Huber, 1987) with parallel isogons (Figure 4.4(c) and (d)). F_3 fold hinges remain relatively straight, as they are the last major folding event that has had an effect on the Willyama rocks in the field area. The F_3 folds verge to the north and northern limbs become overturned, however folds remain upward facing (Figure 4.4(b) and cross section 2). The overturned limbs give the S_2 fabric its southeast trend. The stereographic plot of L_2 and L_3 lineations in sub-area B indicates F_3 folds in the field area are the result of shearing and some homogenous strain (Figure 4.6)(Ramsay and Huber, 1987). This is consistent with the regional interpretation of OD_3 as a folding and shearing event.

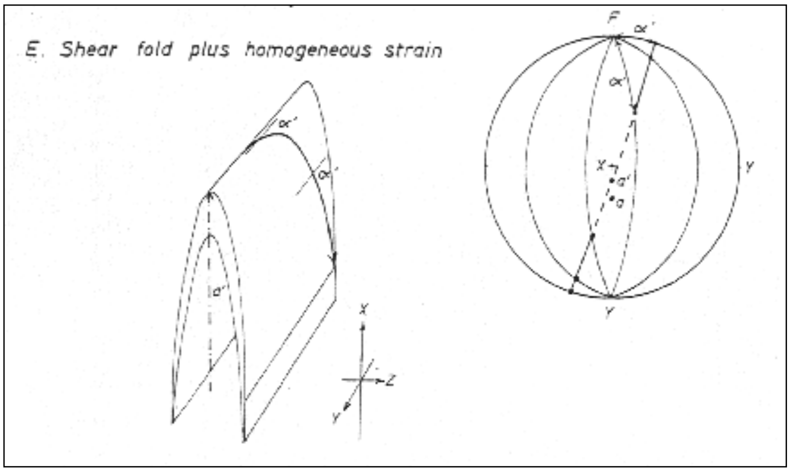

Figure 4.6. Deformed lineation loci: lineation geometry arising during folding of an intially planar surface which contained an initially rectilinear structure. X, Y, and Z indicate the principle strain axes of the superposed homogeneous strain, *a* is the slip direction of simple shear in the shear fold and *a'* the modified direction after imposing a homogeneous strain. (Ramsay and Huber, 1987)

Figure 4.4

(a) Open F_2 folding in psammopelitic gneiss with interbedded migmatite unit, plunging east in the interference zone (subarea B).

(b) Tight F_3 fold in psammopelitic gneiss with interbedded migmatite unit, plunging east and verging to the north.

(c) Sample containing a small F_3 fold and shearing. The plunge of the fold is defined by the rodding lineation of the migmatite around the rim of the sample.

(d) Fold isogon analysis of the fold from (c). It shows the fold is class 2 (Ramsay and Huber, 1987) with parallel isogons.

(e) Thin section from the limb of the fold in (c). It shows the F_3 axial planar fabric cross cutting the stronger S_1 schistosity (micro-graph width approx. 4.5cm; X-polars).

(f) F3 crenulations in the hinge schist unit plunging east at approximately 20 degrees. Lens cap is approx. 4cm in diameter.

(g) S-C mylonite from the MacDonald Shear Zone.

Figure 4.4

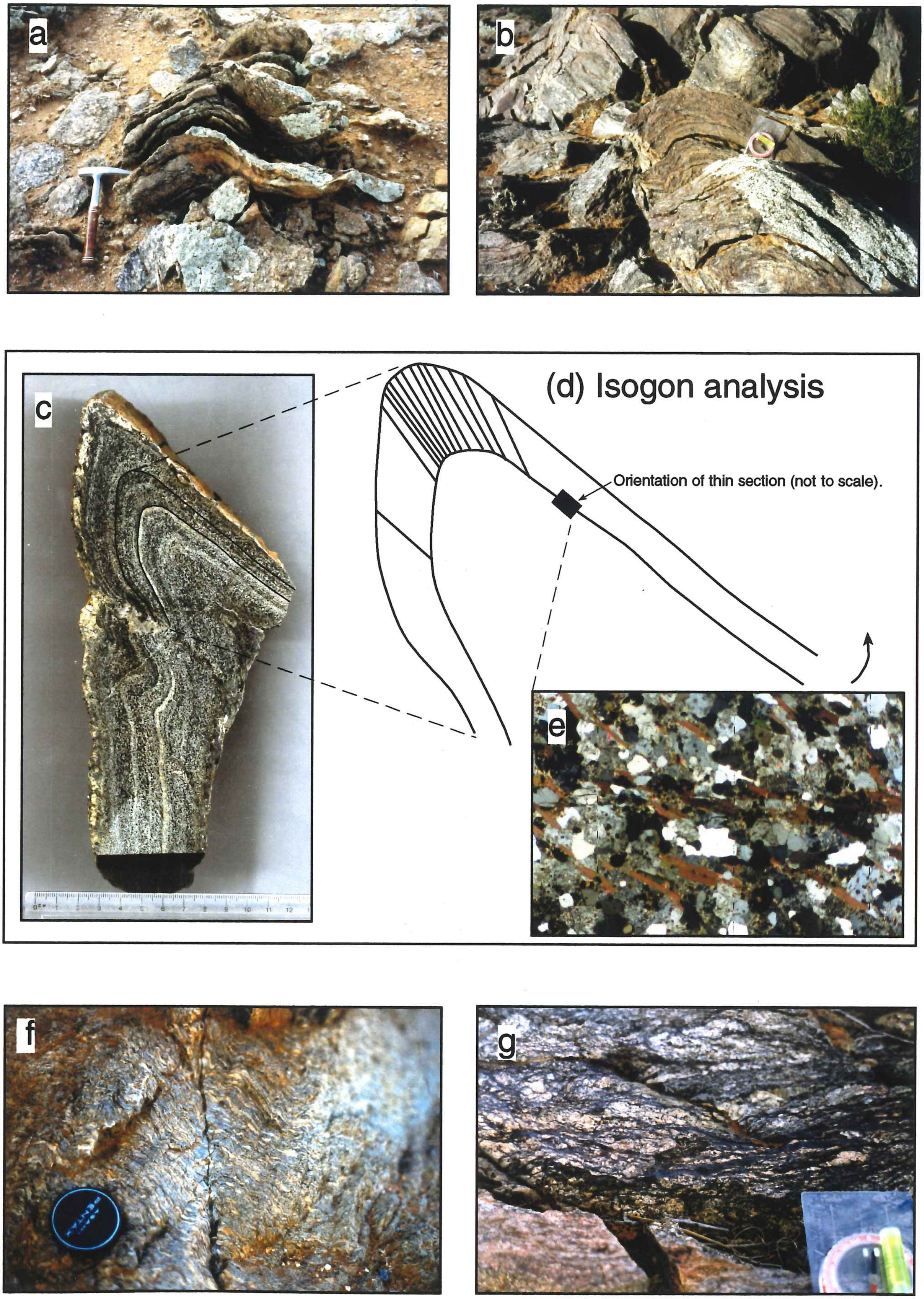
a
b
c
(d) Isogon analysis
Orientation of thin section (not to scale).
e
f
g

Cross section 2. North - South schematic cross section of the 'Woman-in-White' area

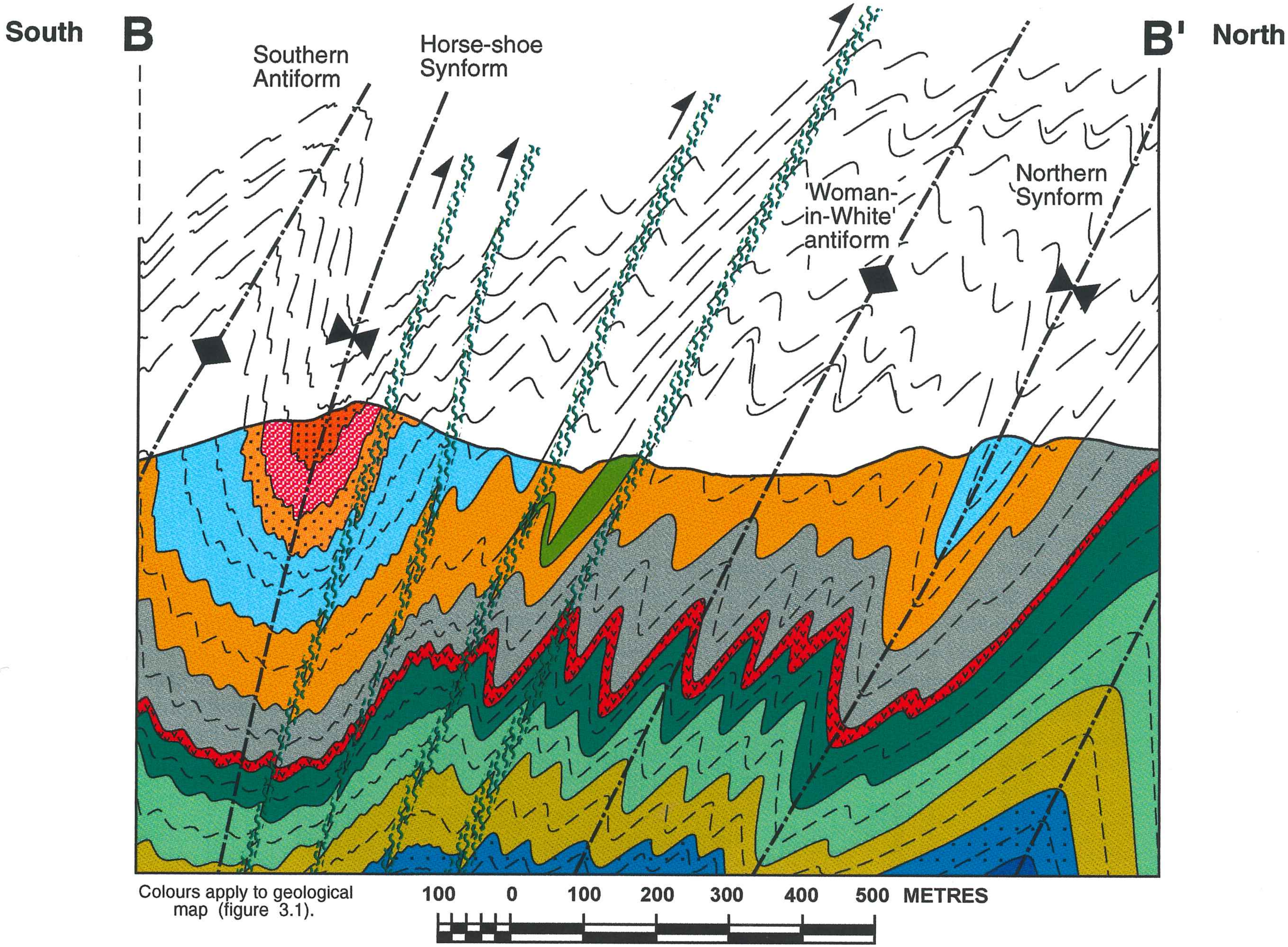

Colours apply to geological map (figure 3.1).

Figure 4.5. Sub areas with L3 lineation data.

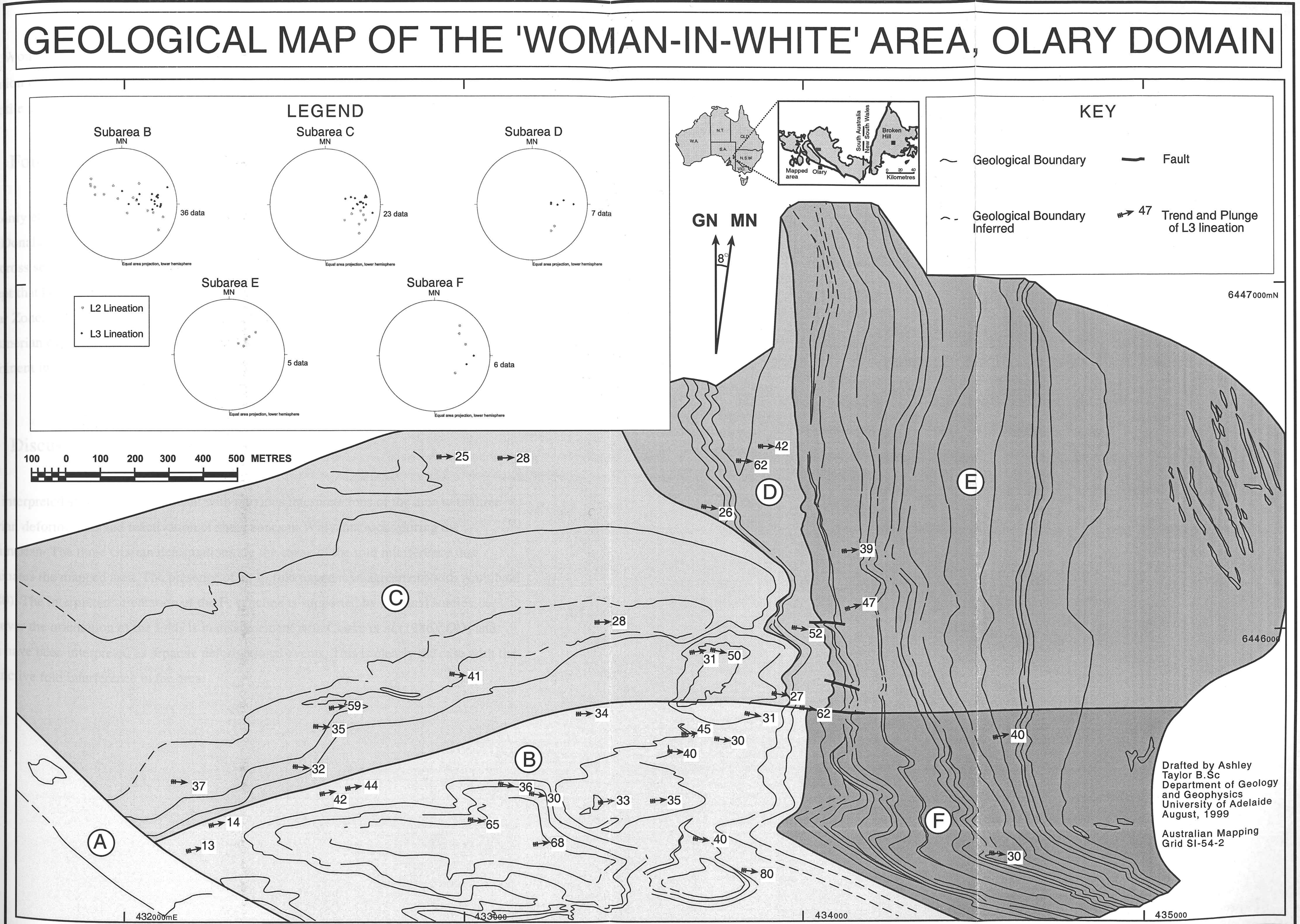

The 'Woman-in-White amphibolite' shows a distinct S_3 fabric trending east (~070 - 090). The foliation is defined by the alignment of subhedral to euhedral grains of blue-green hornblende ± biotite and magnetite.

4.5 Fourth and Fifth Deformations (*D*D_4 and *D*D_5)

The only effect of Delamerian deformation seen in the field area was shearing. The MacDonald Shear Zone in the southwest being the most prominent of these (Figure 4.4(g) and cross section 1). The Adelaidean stratigraphy was relatively undeformed in that region except that bedding was vertical. The strike follows in the same direction as the MacDonald Shear Zone. The Willyama complex rocks did not show any recognisable evidence of Delamerian overprinting except for reactivation of existing shear zones. This is especially prominent in the shear zones to the north (see Clark, 1999) and south of the immediate map area.

4.6 Discussion

The interpreted structure is concordant with previous interpretations of the area with three Olarian deformations and reactivation of shear zones in Willyama rocks during the Delamerian. The three Olarian deformations are the cause of the fold interference that dominates the mapped area. The presence of an F_1 fold nappe is in agreement with Archibald (1980). The interpreted orientation of the F_1 syncline is supported by regional studies, however the orientation of the folds is in disagreement with Clarke *et al.*(1986). *O*D_2 and *O*D_3 have been interpreted as separate deformational events. This is clearly the case with the distinctive fold interference in the area.

CHAPTER 5 - Description of Fold Interference

5.1 Introduction

As mentioned earlier the structure of the area adjacent to the 'Woman-in-White amphibolite' is very complex. The area displays a luniform nature to its geometry. The outcrop evidence for the large-scale structures is abundant in many places. This chapter reviews the evidence for fold interference and describes the interference patterns at different scales.

5.2 Review of Polyphase Folding

Many of the fold structures found in orogenic areas generally show substantial geometric complexity, and it is normal to find that fold forms show complications in three dimensions that are due to the superposition of folding instabilities on pre-existing sets of folds (Ramsay and Huber, 1987).

In many continental regions the crust may be separated into a basement, frequently containing effects of deformation obtained during earlier orogenic events, unconformably overlain by a sequence of flat lying or gently dipping sediments. When a rock arrangement such as this is acted upon by compression the cover sediments may develop regular and somewhat gentle fold structures, however, the contraction of the basement may not be able to be accommodated by reactivation of the pre-existing structural forms. New structures are consequently formed which are superposed on the earlier folds, and these new structures are controlled, both in orientation and in style, by the anisotropy existing before their formation (Ramsay and Huber, 1987).

Another type of superposed folding originates when the principal stress directions change during the history of development in an orogen. This is a common occurrence in all orogenic zones, especially in those sections where the total crustal compression has been large. This type of polyphase deformation may occur either as a result of the action of single pulses of shortening separated by periods of rest and no crustal displacement, or as the result of detachment of a regional deformation into zones where shortening is being accommodated by body translations and body rotations, and other regions where the shortening is taking place by internal deformation (Ramsay and Huber, 1987).

At any particular location the intervals of translation without strain and those periods of active deformation can vary with time, and this results in local discrete and superposed shortening and folding events. Local deformation events which can be separated on geometric information are commonly allocated abbreviations such as D1, D2…Dn. It is generally discovered that the time scale of such polyphase deformations is of the order of tens of millions of years (Ramsay and Huber, 1987).

With a time period of this kind between the principal deformation phases, the temperature and pressure conditions at any one locality have the opportunity to vary. The deformation type and the rock's mineral stability are usually controlled by the metamorphic conditions acting at the time of the individual deformation phases, and the following structural forms are generally identified by specific types of metamorphic fabric fingerprint and particular mineral assemblages (Ramsay and Huber, 1987).

A third class of superimposed folding takes place at the same time as a single progressive deformation as a consequence of smooth and systematic changes of stress and incremental strain during deformation. A constant succession of advancing strain changes can lead to complex shortening and lengthening in a layer and a range of diversely oriented folds and boudinage features may result (Ramsay and Huber, 1987).

In areas that have undergone multiple deformation events there is often an interference pattern present that is commonly more complex than structures produced by single deformation. Because of their likeness to the patterns caused by the intersection of two sets of waves, they are called interference patterns (Ragan, 1973). The appearance of such structures in outcrop depends on the number of generations of folds, on the relative orientations and sizes, and on the orientation of the interference pattern with respect to topography (Hobbs et al., 1976). There are generally four main types of interference patterns (Figure 5.1) even though the spectrum of possible interference pattern geometry is very wide.

(a)

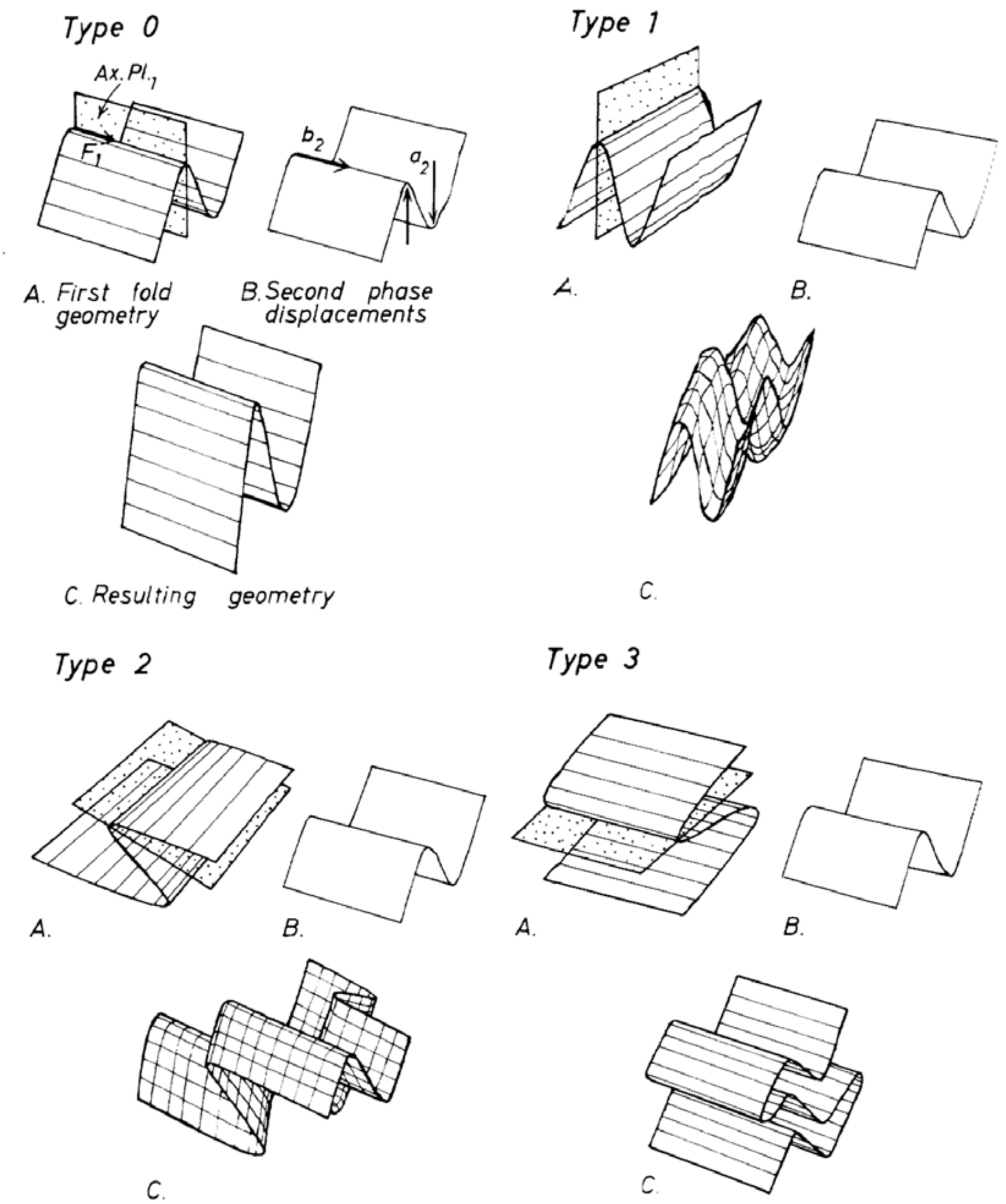

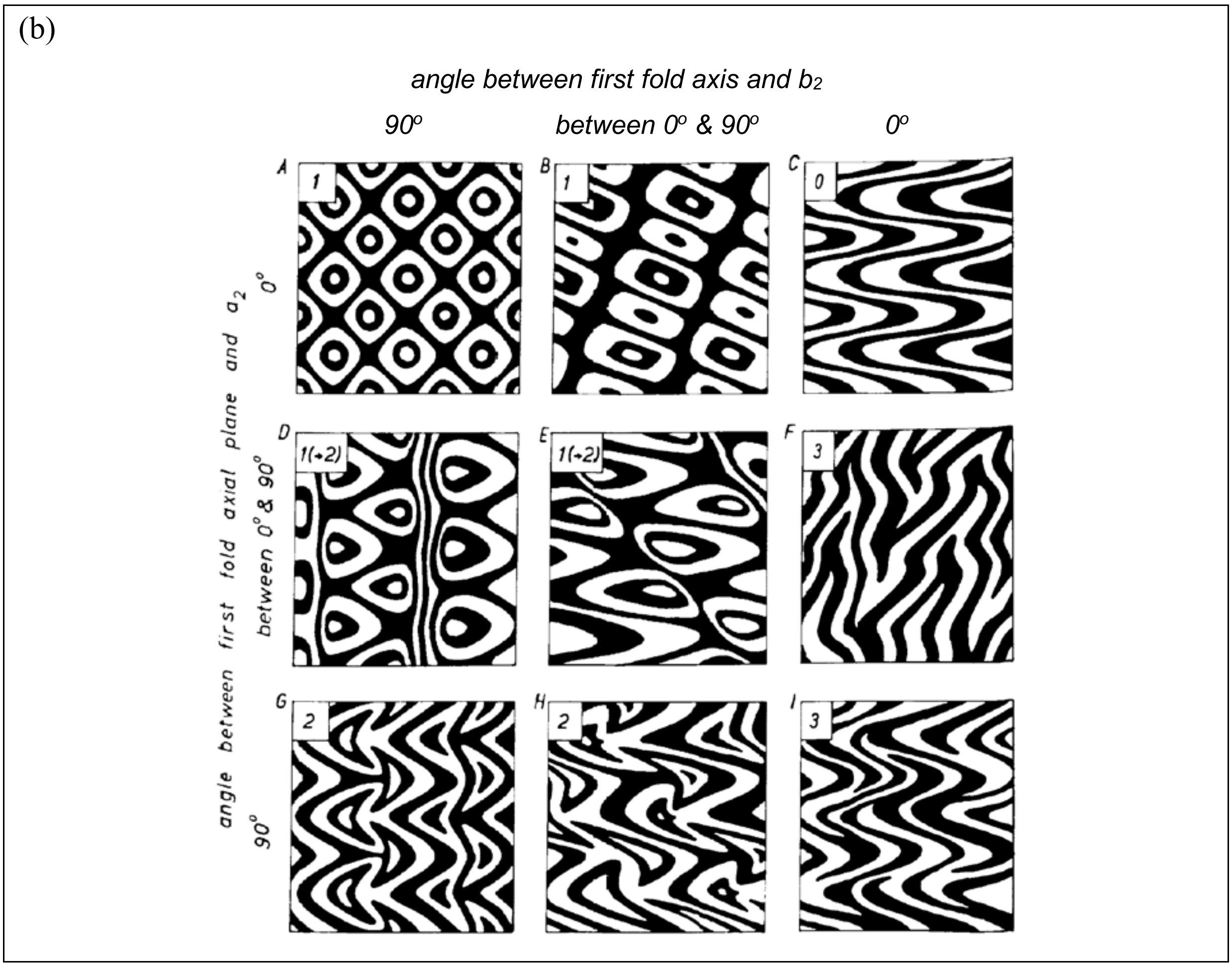

Figure 5.1 (a) The four principle types of three-dimensional fold forms arising by the superposition of shear folds on pre-existing fold forms. (b) Summary of the main types of two-dimensional interference patterns resulting from the horizontal sectioning of the three-dimensional forms. The type numbers are shown in the top left of each box (Ramsay and Huber, 1987).

The names of the four types of patterns are;

- Type 0: Redundant superposition;
- Type 1: Dome-basin pattern;
- Type 2: Dome-crescent-mushroom pattern, and;
- Type 3: Convergent-divergent pattern.

There are many types of structures that are present in areas of polyphase folding and deformation. They have many different forms of formation as well. One of the difficulties in studying such regions is relating the different macro and microstructures to a given deformation event on the basis of style or orientation. It is clear that style and development of structures vary greatly between different rock types and that attention must be paid to the metamorphic assemblages defining each mineral lineation (Harris, 1985). However it is possible determine much of the geology in complex areas by looking at the structure at large and small scales.

5.3 Small Scale Interference

There are the presence luniform patterns on many outcrops in the southern section of the map. Figure 5.2 (a-e) shows different patterns of fold interference. The most common types of pattern are type 2, dome-crescent-mushroom patterns, and type 3, convergent-divergent patterns (Ramsay and Huber, 1987). Most of the patterns are found in psammopelitic schists and gneisses. Some are found in the laminated feldspar and calcsilicate rocks but their abundance is much less. Figure 5.1(c) shows a small luniform pattern in laminated feldspar-biotite rock. This is due to interference of F_2 and F_3 folds. A detailed study of the area surrounding this rock is included in chapter 5.4.

Figure 5.2(d) shows the area interpreted as being affected by all three Olarian Deformations. It is also from the southern interference zone (subarea B). A sample from this area has been analysed in three dimensions in figure 5.3. This rock was sliced into serial sections in an east-west direction (along the L_3 lineation). On the sections is evidence of two fold generations with luniform patterns and many fold closures. This has been interpreted as the interference of F_1 and F_2 folds. Later F_3 folds have themselves folded these patterns. This can be seen in the three-dimensional exploded view of two of the boundaries where the east-west trending F_3 fold has curved the hinges of the earlier folds.

5.4 Mesoscopic Fold Interference

Examples of fold interference at the mesocopic scale were also plentiful. Schist and laminated feldspar units showed the most prominent interference in the southern zone. Figure 5.4 (a-h) shows a grid map carried out in laminated feldspar-biotite rock in the main interference zone. The area was studied in detail after the discovery of the small luniform pattern seen in Figure 5.2(c).

Figure 5.2

(a) Small dome interference pattern in psammopelitic gneiss with interbedded migmatite unit.

(b) Luniform pattern found in laminated feldspar-biotite rock in the main interference zone (Subarea B).

(c) Small luniform pattern found in laminated feldspar-biotite rock. This discovery led to detailed grid mapping of the area surrounding this pattern (see Figure 5.4).

(d) This photo is taken in the calc-silicate unit in an area that has not been severely altered. This has preserved the fold interference patterns seen. This is the area where the layered sample was collected for 3D analysis (see Figure 5.3)

(e) Small luniform patterns found in the psammopelitic gneiss with interbedded migmatite unit.

(f) Psammopelitic gneiss with interbedded migmatite unit from the northern area of the map. This provides evidence for a large dome in that area.

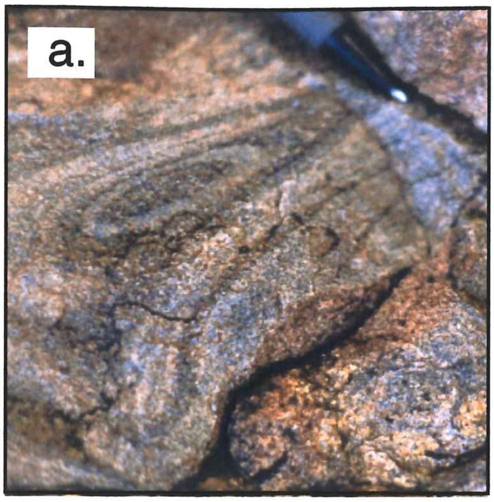

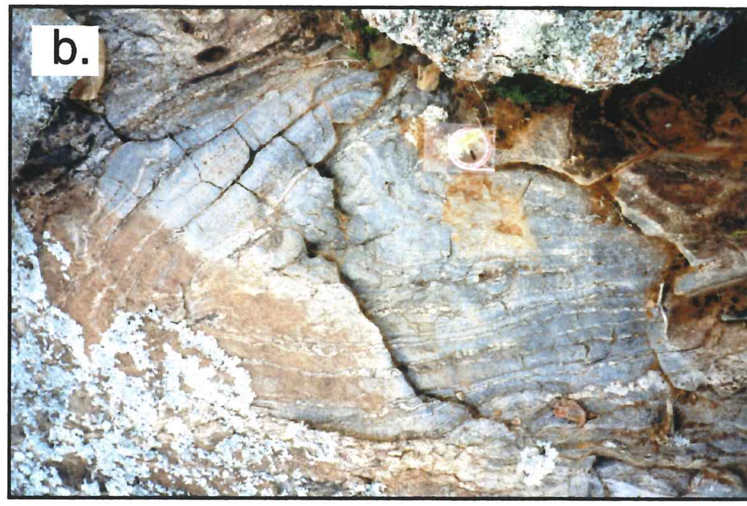

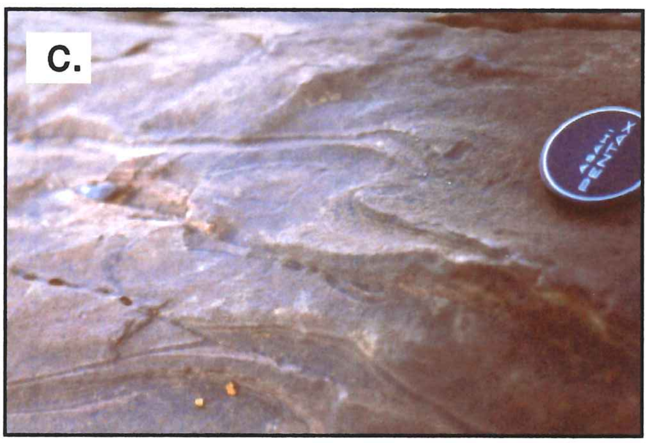

Figure 5.2

Photos showing various fold interference patterns

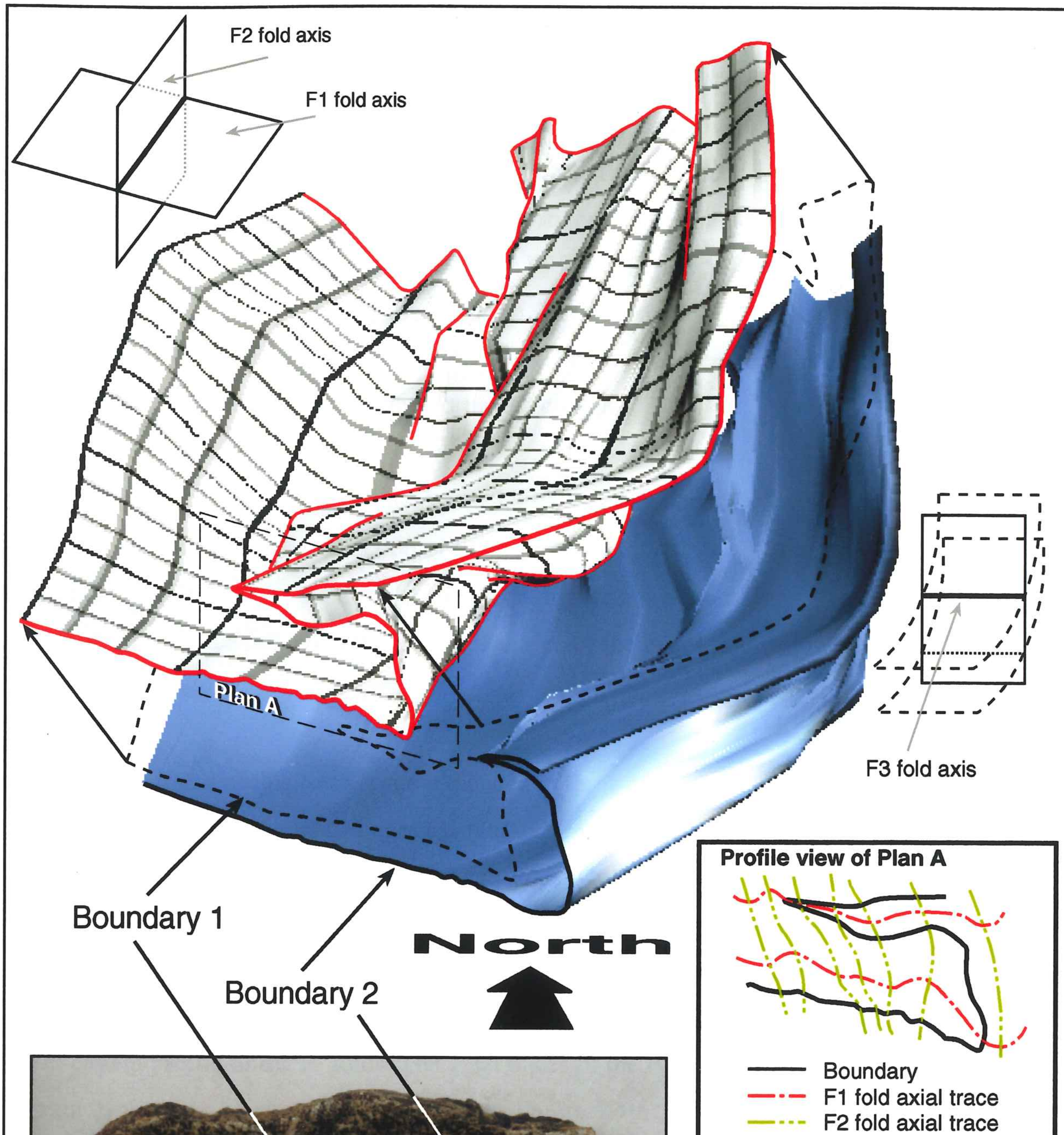

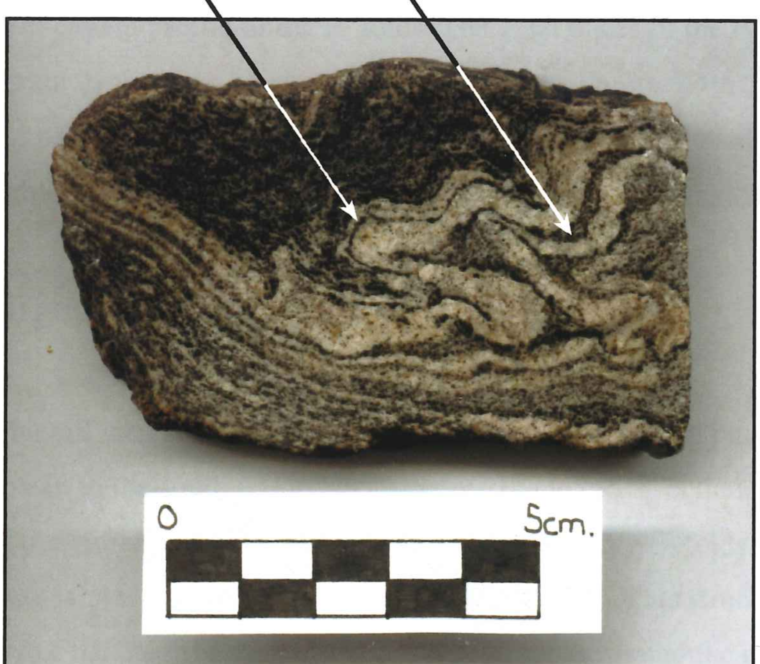

Figure 5.3.

Three dimensional expanded view of two boundaries from the layered sample. The photo inset shows one of the serial sections of the rock from which the profile was constructed. The orientation of the three fold axial planes are also shown.

Figure 5.4(a) shows the shape of the outcrop in grey and all bedding and lineation data collected. The map area was divided into a grid with sides 5m long (overall map is 30x40m). The areas under cover have been inferred in Figure 5.4(b). Trend of bedding has also been added to this map to show the general strike and give shape to the small domes and basins. The abundant fold axes trending to the southeast are F_2 folds. Figure 5.4(c) shows where possible marker boundaries or horizons may outcrop. This too shows the shape and abundance of the small interference patterns. The darker units are interpreted as reflecting the older areas such as in the large dome in the northwest corner.

Analysis of the plunge variation begins in Figure 5.4(d). Contours of 15° increments are shown. This shows the shape and direction of trend of the F_3 fold hinges. They appear to be plunging to the east, which is typical of the field area. Figure 5.4(e) then shows the position of the interpreted F_3 fold axial traces. The overall shapes of the F_3 folds are shown in the three-dimensional analysis.

The remaining diagrams of this section show the area in three dimensions. Figure 5.4(f) is an oblique view that shows the general shapes the major domes and basins. The north-south trending lines of the grid show the profile of the F_2 folds while the east west trending lines give an idea of the variation in plunge. This view also shows the major F_2 folds relaying each other with areas of small scale and large scale folds. This is quite typical of F_2 folds in the field area as mentioned in chapter 4. Figure 5.4(g)is a view of the area looking west. This gives an excellent profile of the F_2 folds. The axial traces of the F_2 folds have been added to this diagram to show the orientation of the F_2 folds. Figure 5.4(h) is another view that shows the shape of the F_3 folds. An interpreted F_3 sketch is also included showing the southern side to be high and the northern side low with some smaller warping in the centre.

5.5 Large Scale Interference

On the overall map scale there are numerous examples of fold interference. The main area is a large basin to the south of the map (subarea B and cross sections 1 and 2). This basin is the result of the Horseshoe Synform refolding north trending F_2 folds (Figure 5.5). Within this basin there is more interference, as seen in section 5.3. This structure is shown best by the boundary of the calcsilicate unit, which is continuous around the rim of the basin. To the east

FIGURE 5.4. CALC-ALBITE GRID MAP WITH FOLD INTERFERENCE

(a) Out crop shape and structural data (So and S1).

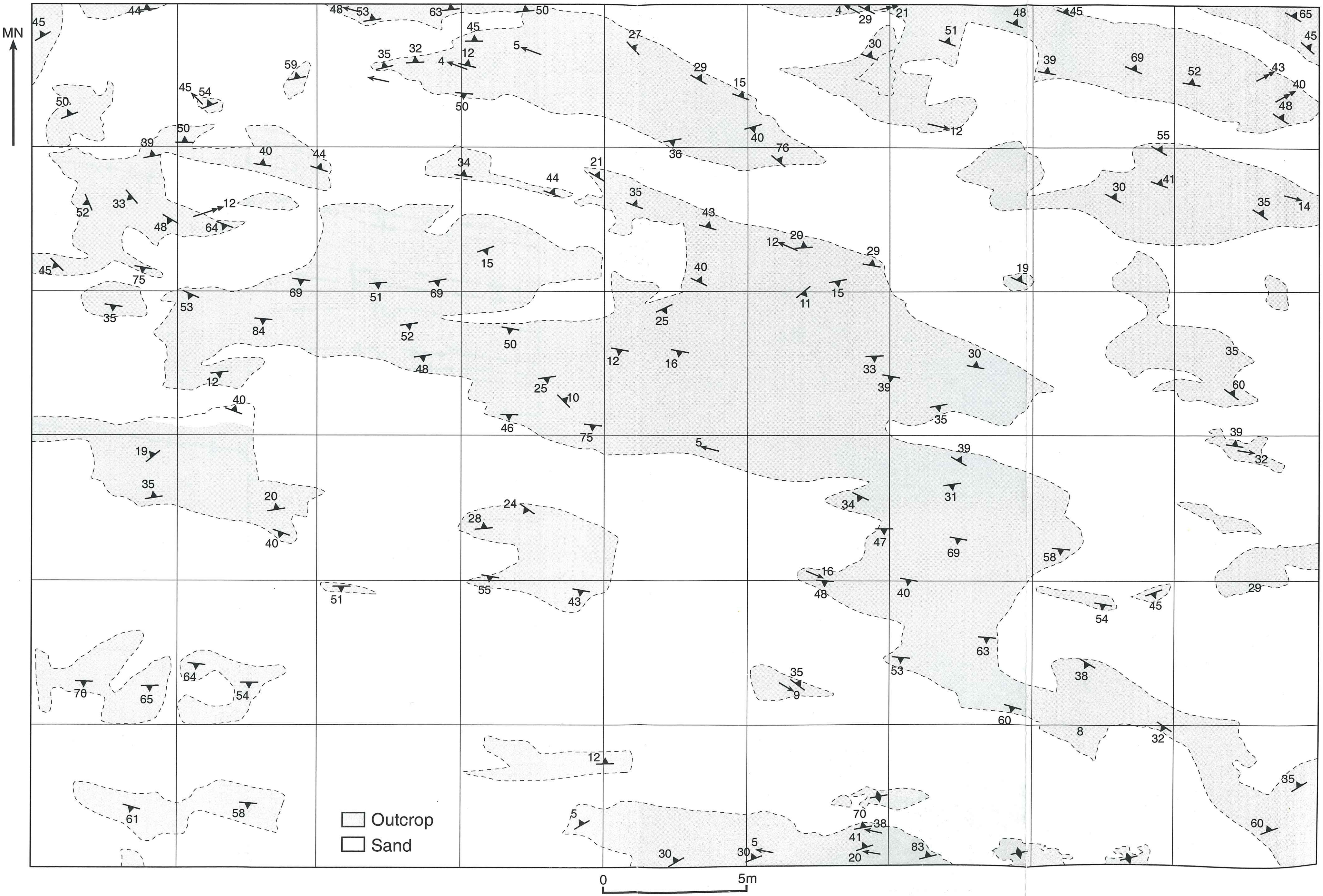

FIGURE 5.4. CALC-ALBITE GRID MAP WITH FOLD INTERFERENCE

(b) Inferred fold axial traces and trend of bedding (So).

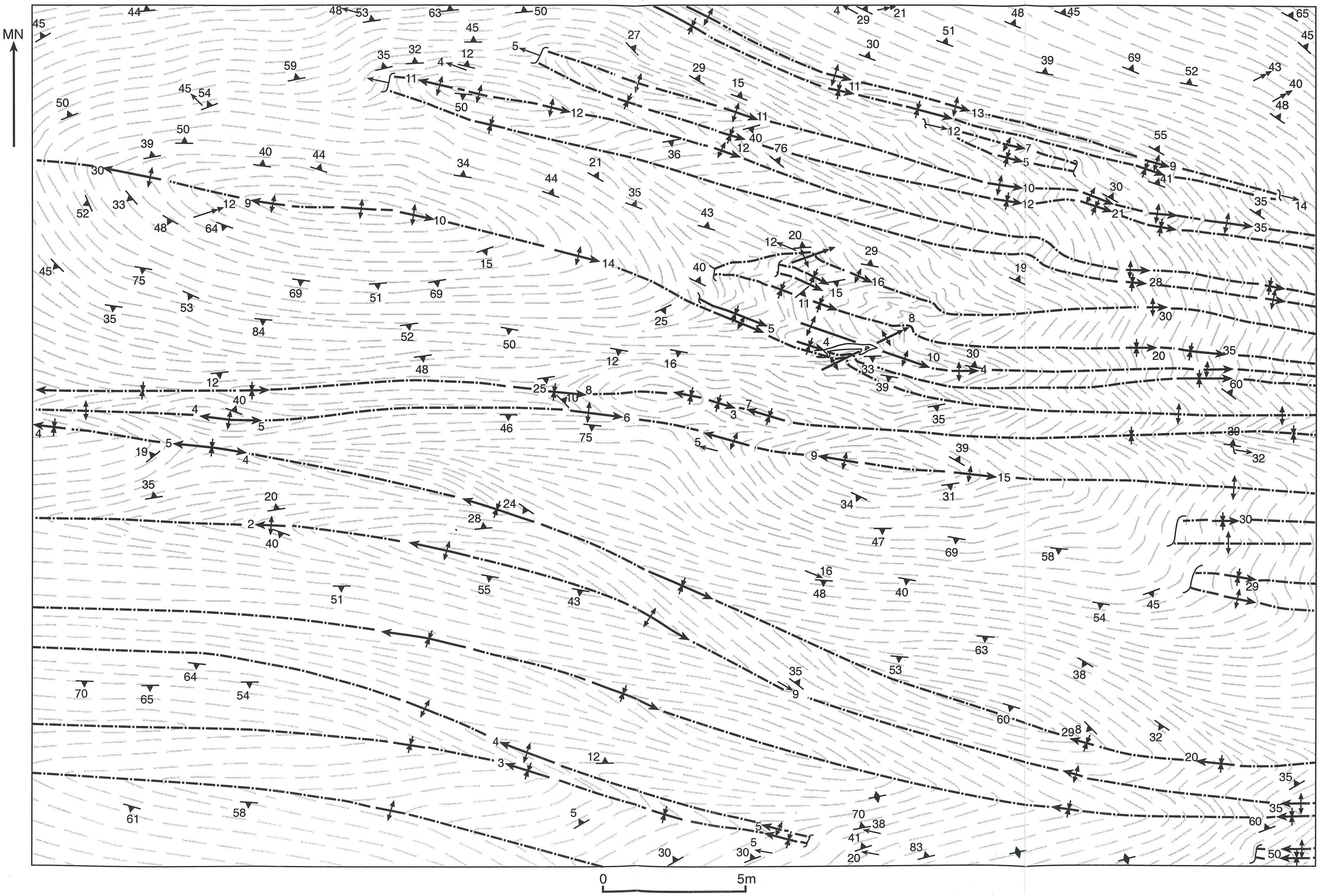

FIGURE 5.4. CALC-ALBITE GRID MAP WITH FOLD INTERFERENCE

(c) Possible boundary or thin horizon positions (darker layers are oldest).

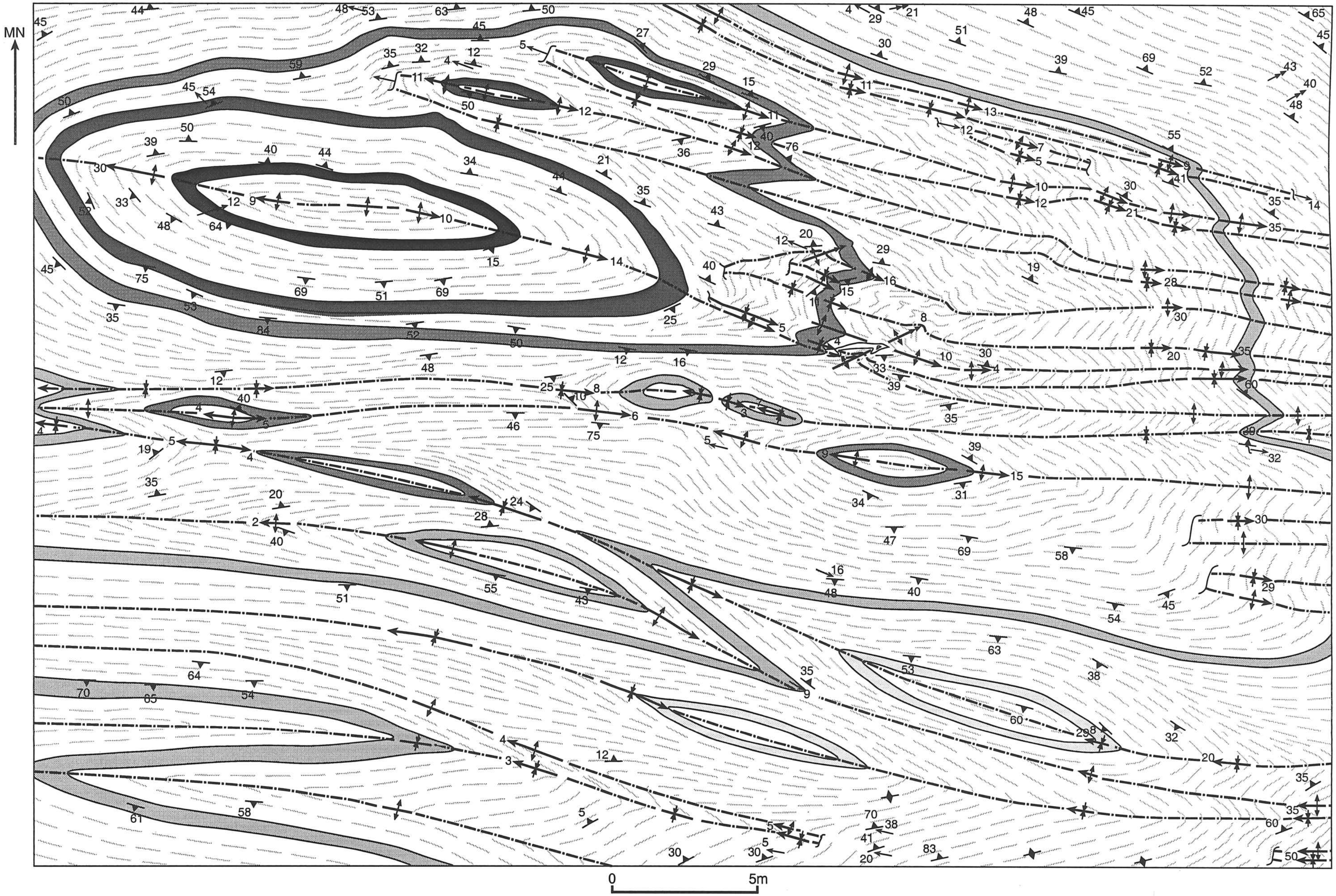

FIGURE 5.4. CALC-ALBITE GRID MAP WITH FOLD INTERFERENCE

(d) Contours of plunge of F_2 fold hinges and L_2 lineations.

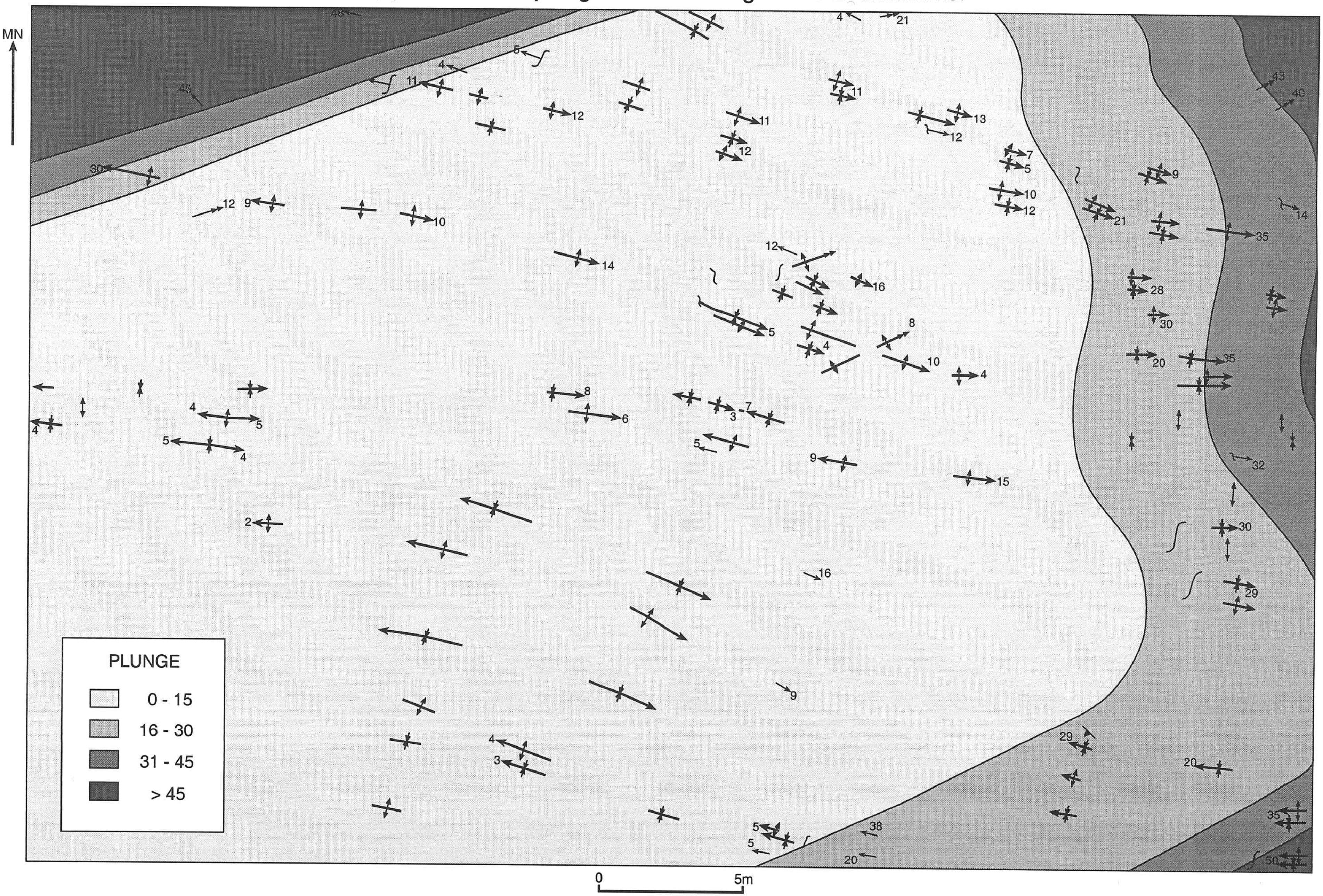

FIGURE 5.4. CALC-ALBITE GRID MAP WITH FOLD INTERFERENCE

(e) Interpreted F_3 axial traces.

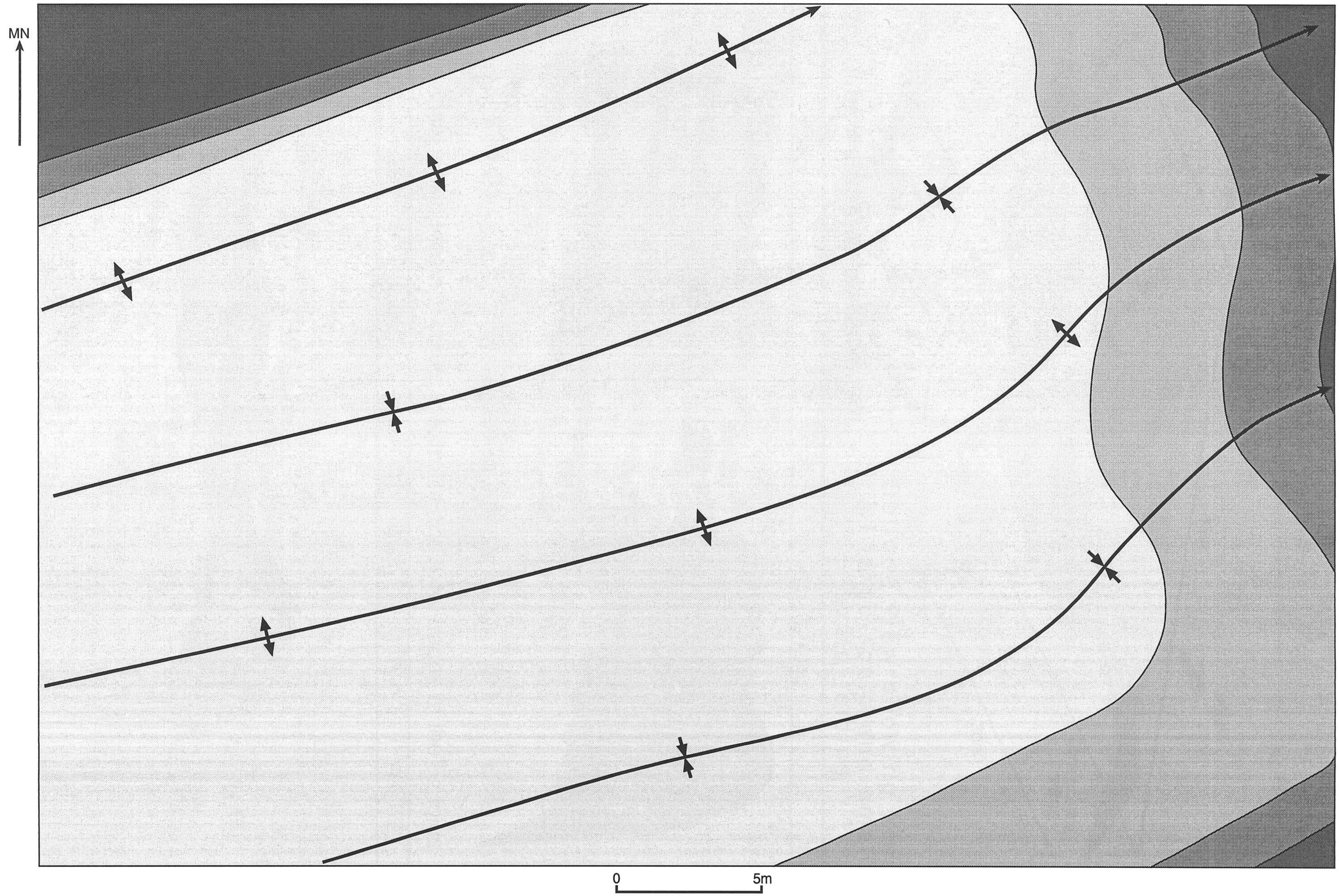

Figure 5.4 Three dimensional analysis

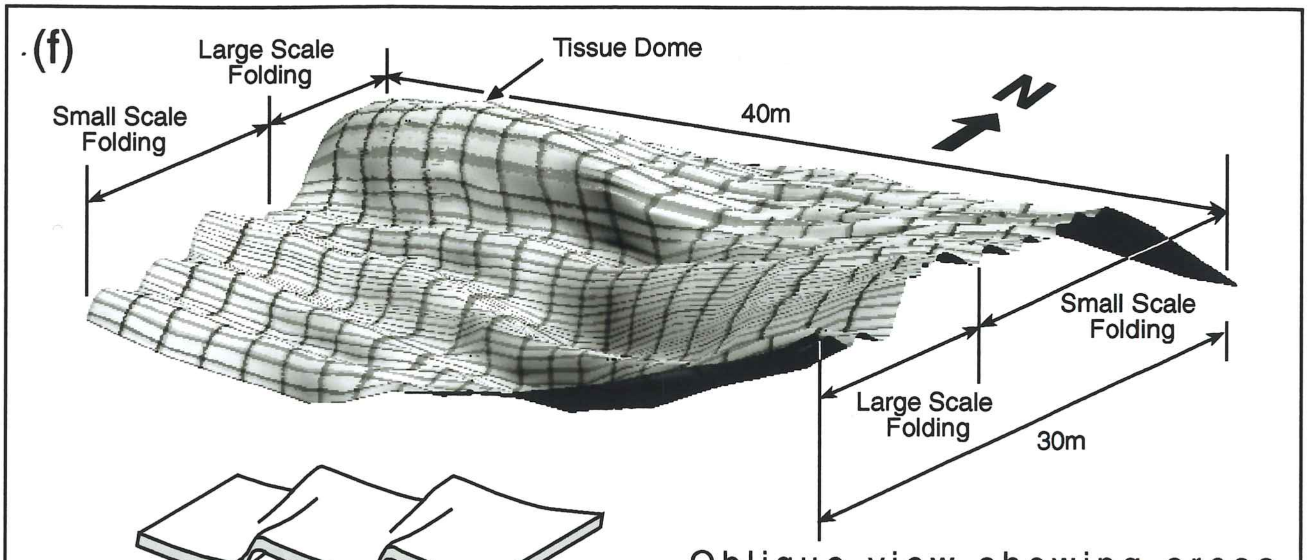

Oblique view showing areas of large scale and small scale folding

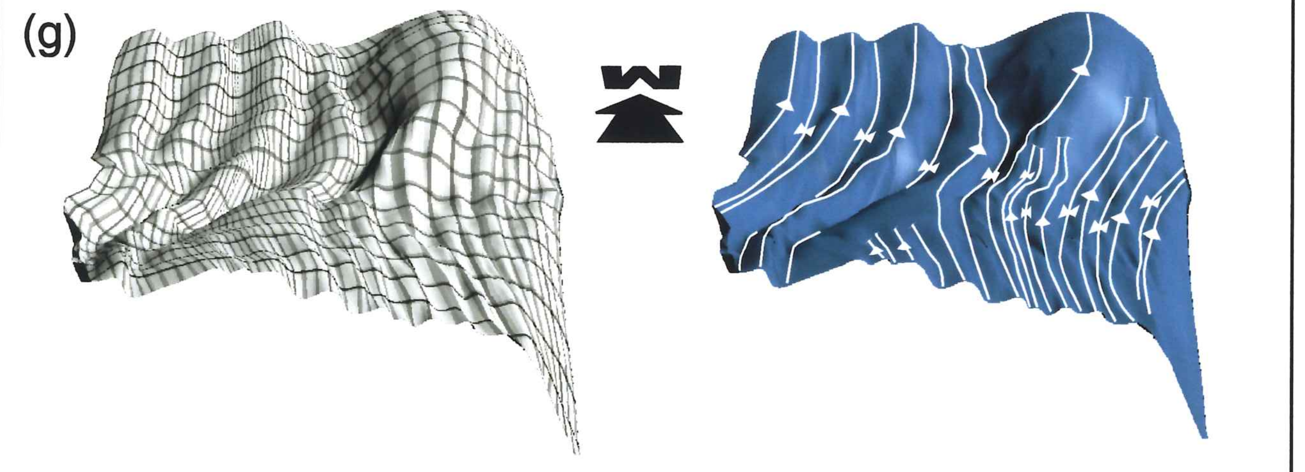

View looking west showing the profile and axial traces of the F_2 folds

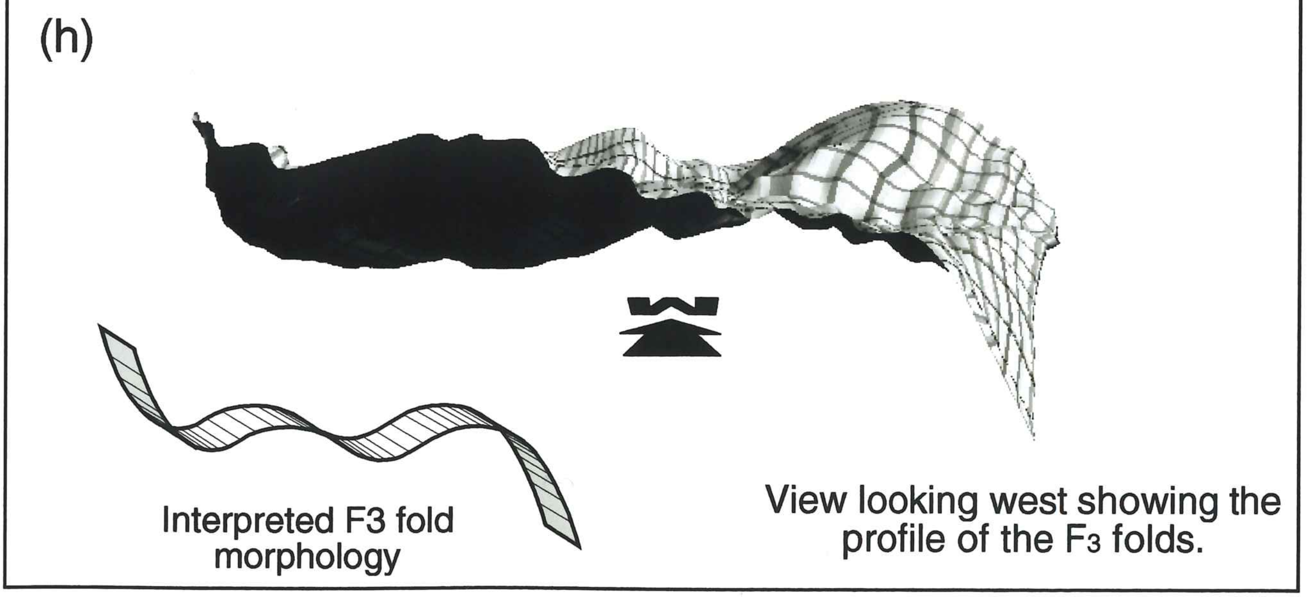

View looking west showing the profile of the F_3 folds.

Figure 5.5 Fold axial traces of major F1, F2 and F3 folds.

GEOLOGICAL MAP OF THE 'WOMAN-IN-WHITE' AREA, OLARY DOMAIN

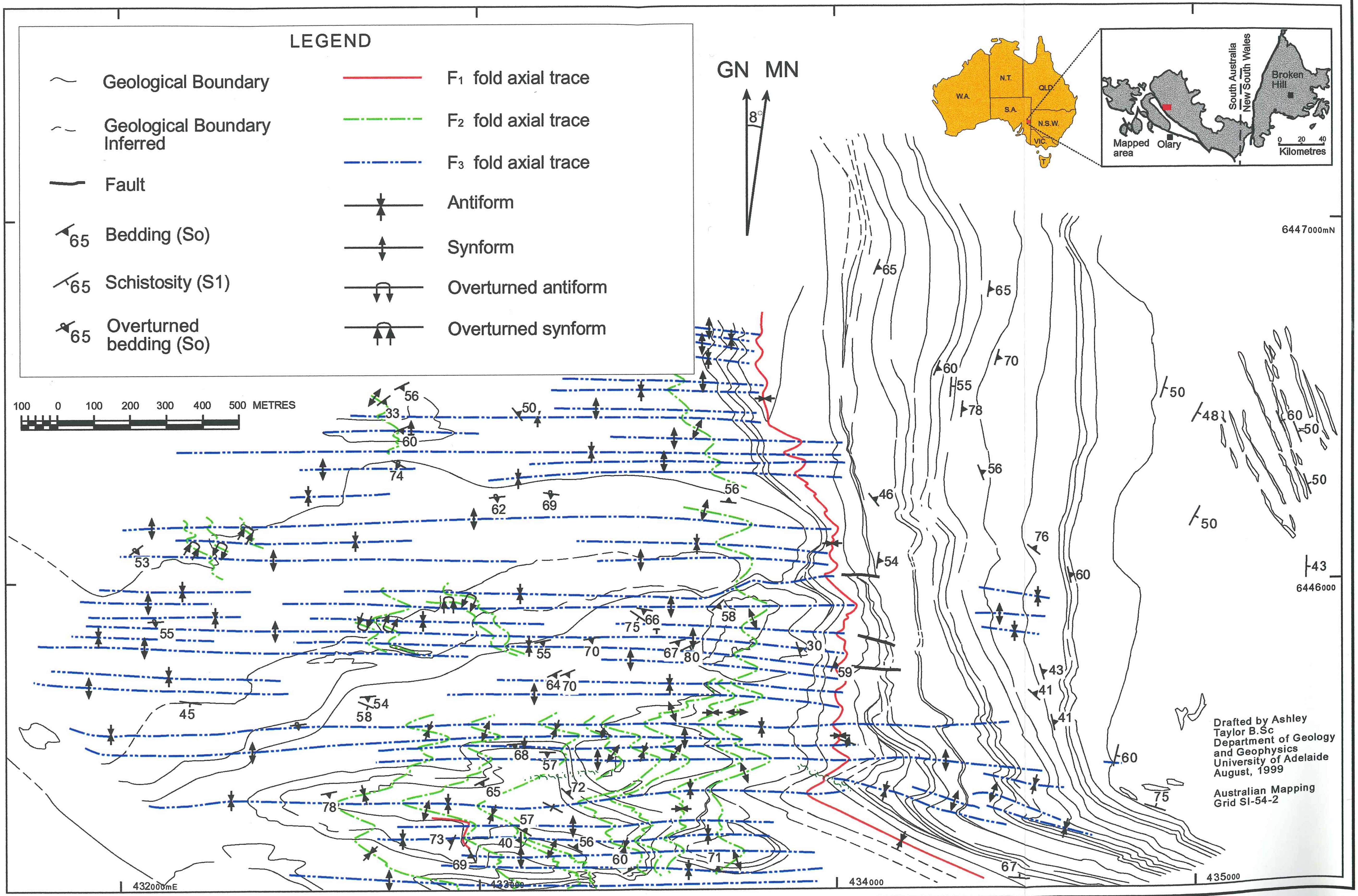

of this structure are more slightly smaller interference patterns that cause the repetition of the laminated feldspar rock (LFR). This is also due to the interference of F_2 and F_3 folds (Figure 5.5). This interference is the cause of the separation of the main WIWA within the LFR unit. These patterns are of type 2 and type 3 once again (Ramsay and Huber, 1987). In the north of the map area another zone of interference is present. Archibald (1980) interpreted a large dome (500m) in diameter to exist at that location. The field area of this study only covered the very southern extent of this dome however there is plenty of evidence for fold interference as shown by the sample in Figure 5.2(f).

5.6 Discussion

Fold interference in the field area is present on all scales. The effects of OD_2 and OD_3 especially have given the flat-lying western limb of the F_1 fold a luniform, dome and basin morphology. Detailed study of individual outcrops confirm that discontinuity of lithologies observed at map scale is due to fold interference. The eastern side of the F_1 syncline does not show the same level of fold interference as that on the western side. Only isolated examples can be found in the field. Ramsay and Huber (1987) type 2 and type 3 patterns are the most common in the area mapped. The presence of both is due to the angle between OD_2 and OD_3 compression, which is approximately 40° in the main interference zones.

CHAPTER 6- Tectonic Model

6.1. Introduction

The structural analysis in chapter 4 suggested the presence of an F_1 synform with the axial trace striking north south and vergence to the west. As an axial planar fabric, the S_1 layer parallel schistosity has been suggested to be due to the synform. The formation of this fold nappe is the focus of this chapter in describing a tectonic model for the formation of the 'Woman-in-White' area.

6.2 Tectonic Model for the 'Woman-in-White' Area

The Willyama Supergroup has been interpreted as having been deposited in a failed Palaeoproterozoic rift, which was subsequently deformed and metamorphosed. The western margin of the rift, between Mount Robe and Olary, corresponds with the western limit of significant volumes of basic magma (Flint and Parker, 1993) and granitoids that intruded the area (Figure 6.1). Constable (1999) has interpreted the granitoids to intrude before OD_1, and hence they have undergone the same amount of deformation as the Willyama Supergroup Metasediments (Figure 6.1).

The first stage of the tectonic model is during the Mesoproterozoic. This is the time of the deposition of the Willyama Supergroup sediments, volcanics on top of Archean Basement. This is also the time of the intrusion of pre OD1 granitoids into the Willyama Supergroup metasediments (Figure 6.1(a)).

The second stage of the tectonic history begins with the onset of the Olarian Orogeny. This produced thin sheet thrust stacking and crustal thickening along with basement thickening (Figure 6.1(b)). For thrust stacking to occur there needs to be the presence of a decollement layer which is generally a horizon which is incompetent providing a plane of weakness. The thrust sheets would have been transported to the west onto a foreland Archean shelf.

As the Olarian Orogeny continued, early basement extensional faults were reactivated as thrust sheets (Figure 6.1(c)). This led to the formation of fold nappes verging to the west with

Figure 6.1: Proposed Tectonic Model for the Olary Domain

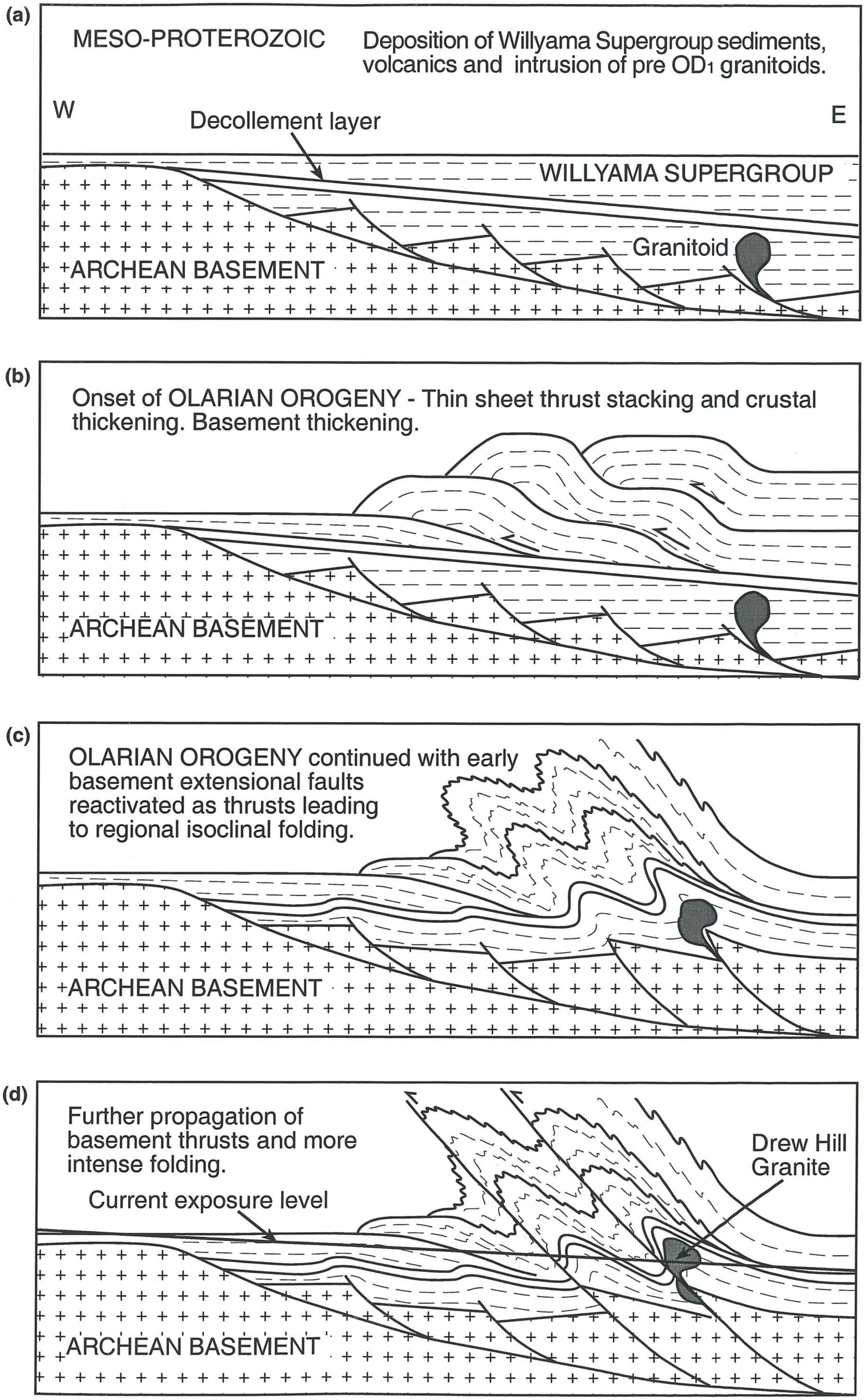

Adapted from Menpes (1992) for the Willyama Complex limbs becoming overturned. This is the explanation for the formation of the F_1 synform in the 'Woman-in-White' area, which has closure to the east and vergence to the west.

Further propagation of basement thrusts led to more intense folding (Figure 6.1(d)). This folding event is attributed to OD_2, which refolded the F_1 recumbent terrain to produce structures such as those found in the 'Woman-in-White' area. The propagation of the basement thrusts and erosion led to the unearthing of pre OD_1 granitoids, such as the Drew Hill Granite, found in the 'Woman-in-White' area.

6.3 Delamerian Analogue

Menpes (1992) is a study of the structural evolution of a transpression zone in the southern Adelaide Fold Belt. It is suggested that the incompetent units of the Normanville Group sediments acted upon by a shear zone formed the basal decollement to thin-skin thrusting. The thrust sheets were then carried across the decollement to the foreland consisting of Gawler Craton rocks. Further transpression led to further propagation of thrusts and the formation of a major fold structure.

6.4 Discussion

A number of complications have arisen with the development of this model. This is because the model is based on a few assumptions. Firstly, the geometry of different Olarian Deformations differs laterally. Also there is a minor oblique component to thrusts in some areas. The different deformation directions can be attributed to external boundary displacements of the structure, and inner rheological variation. The rheological variation is important in the structural description of the 'Woman-in-White' area, and it provides an explanation for the intense fold interference seen on the western side of the F1 synform compared to the relatively uniform eastern limb. Another explanation for this is due to the presence of the Drew Hill Granite, which provided the metasediments with some protection from the later deformation events.

CHAPTER 7- Conclusion

The 'Woman-in-White' area is structurally complex. It has undergone five major deformational events. This includes events OD_{1-3} and events DD_{4-5}. Throughout the area is the presence of a layer parallel schistosity (S_1), which is the axial planar fabric to a large-scale F_1 synform. The axis of the F_1 synform strikes north south and verges to the west causing the eastern limb to be overturned. The eastern limb is only interpreted as overturned due to structural data as no younging directions were found in that area. S_2 is the axial planar fabric to folds that generally trend to the north-east. Axial planar cleavages and fabrics are widespread, however only in areas of F_2 folds. The third deformation was very intense for the 'Woman-in-White' area. Two fabrics represent S_3. There is the axial planar fabric to F_3 folds, which trend consistently east-west. The second type of S_3 fabric is a crenulation of the S_1 fabric.

Interference of the three Olarian deformations has given the 'Woman-in-White' area a ‘dome and basin’ morphology. Evidence for fold interference exists at all scales. The most common interference is due to deformation events OD_2 and OD_3. Only isolated examples of all three Olarian events interfering were found in the study area. The most common type of interference patterns in the 'Woman-in-White' area are Ramsay and Huber (1987) type 2 and type 3 patterns. The most intense deformation and fold interference occurs on the western limb of the F1 synform. The eastern limb has remained relatively uniform due to the presence of the Drew Hill Granite and also to variation in rheological properties.

Three-dimensional analysis was extremely good for interpreting fold interference. It made it easier to classify the fold forms and also to visualise what the layers look like when they are not incised and shown in two dimensions either in outcrop or in theory.

The 'Woman-in-White' area is extremely complex. This made the area very exciting to investigate and analyse, however greater knowledge of the structure of the region could be obtained by further detailed studies.

Acknowledgments

There are many people whom I would like to thank in helping me prepare this thesis. Firstly Primary Industries and Resources of South Australia (PIRSA) for financial backing of the project in covering field and lab costs. Colin Conor (PIRSA) for help in the field and also help in preparing written work. My supervisor Dr. Pat James for help and advice throughout the year. Sherry Proferes for help in drafting maps and Gerald Buttfield for meaningful chats about the weather over the VHF, and Wayne Mussared for producing the thin sections.

Thankyou to the people at RFDS Pt. Augusta for connecting us to Adelaide many times while in the field. Also Ron Baxter for allowing us access to his land, and Malcolm for the company, and more chats about the weather.

Thankyou to the other Olary boys, Jono and Simmo. Six weeks was a long time but with you guys it was an eternity - just joshin'. Thankyou to Michael Szpunar (PIRSA) for help in the field and for directing us to the Democratic Club (Broken Hill)- what a night! Thankyou to all who visited us in Olary, especially John Foden for supplying the red - how 'bout them rissoles! Thankyou also to the "CHAIR" with whom I spent many hours with (mind the creek!) and the guys at Mannahill Pub for their hospitality.

My warmest thanks go to my Gran who has looked after me for the last four years (very well) and also my parents for helping me financially this year. To my fellow Honours students, thankyou for the great year of memories and good luck in the future, and last but no means least, to Alicia who has looked after me extremely well during a very stressful time of year, I give my warmest thanks.

References

Archibald, NJ, (1980). Old Boolcoomata-Mt Mulga Mine Area, Geology. In: Reports on E.L. 263, 416, 450, 457,767, 848, 1175. Esso Exploration and Production Aust. S. Aust. Dep. Mines and Energy. Open file env. 3360 (unpublished)

Ashley, PM, Conor, CHH, Skirrow, RG, (1998). Geology of the Olary Domain, Curnamona Province, South Australia. Field guidebook to Broken Hill Exploration Initiative excursion. Department of Primary Industries and Resources of South Australia. 53pp.

Berry, RF, Flint, RB, and Grady, AE. (1978). Deformation history of the Outalpa area and its application to the Olary Province, South Australia. *Transactions of the Royal Society of Australia*, **102**: pp45-53.

Brett, D, (1998). Structural, geochemical and isotopic investigation of granitoids within the central area of the Eastern Weekeroo Inlier, Olary Domain, South Australia. *B.Sc Honours thesis*. University of Adelaide.

Clark, JL, (1999). Structural and metamorphic investigation of the Cathedral Rock – Drew Hill Area. Olary, South Australia. *B.Sc Honours thesis*. University of Adelaide.

Clarke, GL, Burg, JP, Wilson, CJL, (1986). Stratigraphic and structural constraints on the Proterozoic tectonic history of the Olary Block, South Australia. *Precambrian Research*, **34**: pp107-137

Clarke, GL, Guiraud, M, Powell, R, Burg, JP, (1987). Metamorphism in the Olary Block, South Australia: compression with cooling in the Proterozoic fold belt. *Journal of Metamorphic Geology*, **5**: 291-306

Constable, SA, (1999). Geological mapping and the geochemical and petrological characterisation of the 'Woman - in – White' amphibolite and associated felsic rocks. *B.Sc Honours thesis*. University of Adelaide.

Flint, RB, Parker, AJ, (1993).Willyama Inliers, in Drexel, JF, Preiss, WV, Parker, AJ (eds.) The Geology of South Australia. Volume 1. The Precambrian. *Geological Survey of South Australia*. Bulletin **54**: 82-93.

Hobbs, BE. Means, WD, and Williams, P.F., (1976). *An outline of structural geology*. Toronto, John Wiley and Sons, pp571.

Majoribanks, RW. Rutland, RWR. Glen, RA. and Laing, WP., 1980. The structural and tectonic evolution of the Broken Hill Region, Australia. *Precambrian Research*, **13**: 209-240.

Menpes (1992). Structural evolution of a transpression zone in the southern Adelaide fold belt: Northeast Dudley peninsula, Kangaroo Island. *B.Sc Honours Thesis.* University of Adelaide.

Ragan, DM, (1973). *Structural geology: an introduction to geometrical techniques, second edition.* John Wiley and Sons , Inc. Canada. P208

Ramsay, JG. and Huber, MJ. (1987). *The Technique of Modern Structural Geology. Volume 2: Folds and fractures*. Academic Press London.

Appendix 1- Locality map for cross sections, samples, photos, gridmaps